Diffraction Shader

Bachelorarbeit

der Philosophisch-naturwissenschaftlichen Fakultät
der Universität Bern

vorgelegt von

Michael Single

2014

Leiter der Arbeit:
Prof. Dr. Matthias Zwicker
Institut für Informatik und angewandte Mathematik

Abstract

Inhaltsverzeichnis

Kapitel 1

Introduction

Kapitel 2

Theoretical Background

2.1 Definitions

2.1.1 Diffraction

ADD IMAGES

A wave is the spatial propagating variation or rather perturbation or also an oscillation of a location-and time-dependent physical quantity. In Mathematics, when talking about a wave, we are referring to the so called wavefunction $y(x,t) = Asin(wt - kx)$ which is a solution for the so called wave-equation. In general, this function depends on the location x and in time t. The maximal amplitude / magnitude of a wave is denoted by A. The phase of wave indicates in which part within its period with respect to a reference point in time / location the wave is located. Naturally occurring waves are uncommonly purely monochromatic waves, rather an overlapping of many waves with different wavelengths, which is denoted by interference. Interference is a phenomenon in which two waves superimpose to form a resultant wave of greater or lower amplitude. All portions of these corresponding wavelengths are forming the so called spectrum. For example sunlight which is a overlapping of many electromagnetic monochromatic waves of different wavelengths, ranging continuously from infrared across visible light to ultraviolet. Thereby, many effects may occur like interference - by overlapping two waves they either will amplify or cancel out partially or even totally each other in some location. Waves can experience in a different way a change in their form of appearance through reflexion, transmission, refraction or diffraction. In this thesis we are interested in particular in the bending of waves the so called effect of diffraction, which cannot be modeled using the standard ray theory of light.

When a wavefront is occluded partially by an obstacle, the wave is not only moving in the direction provided by the ray geometry, but also occur complex wave-movements outside of the geometric ray boundaries. This occurrence is called diffraction and occurs on the border of the wave's obstacle.

Generally, the effect of diffraction occurs on the border of obstacle whenever a propagating wave encounters that obstacle. But its effects are generally most pronounced for waves whose wavelength is roughly similar to the dimensions of the diffracting objects. Conversely, if wavelength is hardly similar, then there is almost no diffraction at all. This implies diffraction occurs mostly when the

surface detail is highly anisotropic. If the obstructing object provides multiple, closely spaced openings, a complex pattern of varying intensity can result. This is due to the superposition, or interference, of different parts of a wave that travels to the observer by different paths.

Example: Light rays passing through a small aperture will begin to diverge and interfere with one another. This becomes more significant as the size of the aperture decreases relative to the wavelength of light passing through, but occurs to some extent for any aperture or concentrated light source.

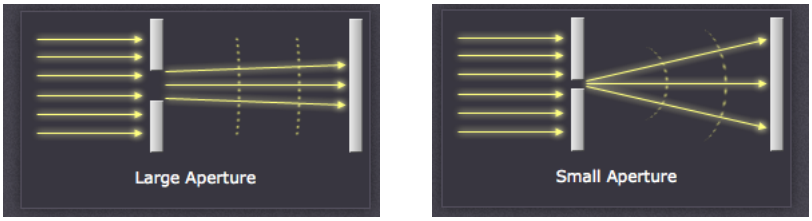

(a) Large Aperture (b) Small Aperture

Abbildung 2.1: Diffraction: Single Slit Example

Since the divergent rays now travel different distances, some move out of phase and begin to interfere with each other — adding in some places and partially or completely canceling out in others. This interference produces a diffraction pattern with peak intensities where the amplitude of the light waves add, and less light where they subtract. If one were to measure the intensity of light reaching each position on a line, the measurements would appear as bands similar to those shown below.

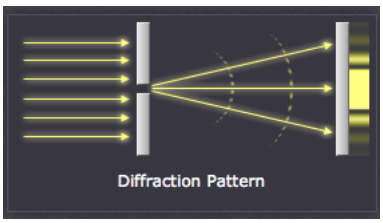

Abbildung 2.2: Diffraction Pattern

In general interference produces colorful effects due to the phase differences caused by a wave traversing thin media of different indices of refraction.

The effects of diffraction are often seen in everyday life. The most striking examples of diffraction are those that involve light; for example, the closely spaced tracks on a CD or DVD act as a diffraction grating to form the familiar rainbow pattern seen when looking at a disk

In optics, a diffraction grating is an optical component with a periodic structure, which splits and diffracts light into several beams travelling in different directions. The directions of these beams depend on the spacing of the grating and the wavelength of the light so that the grating acts as the dispersive element. The relationship between the grating spacing and the angles of the

incident and diffracted beams of light is known as the grating equation. See chapter Evaluation Data Acquisition for further insight.

2.1.2 Radiometry

Light is fundamentally a propagation form of enegry, so it is useful to define the SI unit of energy which is joule (J). To aid our intuition, let us describe radiometry in terms of collections of large numbers of photons. A photon can be considered as a quantum of light that has a position, direction of propagation and a wavelength λ measured in nanometers. A photon travels in a certain speed, denoted by $v = \frac{c}{n}$, that depends only on the refractive index n of the medium through which it propagates and the speed of light c. This allows us do define the frequency $f = \frac{c}{\lambda}$. The amount of energy q carried by a photon is given by the following relationship: $q = hf = \frac{hc}{\lambda}$ where h is the Plank's constant.

Spectral Energy
If there is a large collection of photons given, their total energy $Q = \sum_i q_i$ is the sum of energies of each photon q_i within the collection. But how is the energy distributed across wavelenghts? One way in order to determine this distribution is to order all photons by their associated wavelength and then make a histogram from them. This is achieved by a discretization of their spectrum and combine all photons which will fall into the same interval, i.e. compute the sum for each interval from the energy of all their photons. By dividing such an interval by its length, denoted by Q_λ, we get a relatively scaled interval energy, which is called spectral energy and it is an intensive quantity. Intensive quantities can be thought of as density functions that tell the density of an extensive quantity at an infinitesimal point.

Power
Power is the estimated rate of energy production for light sources and is measured in the unit Watts, denoted by Q, which is another name for joules per second. Since power is a density over time, it is well defined even when energy production is varying over time. As with energy, we are really interested in the spectral power, measured in W/nm, denoted by Φ_λ

Irradiance
The term irradiance comes into place when we are interested in *how much light hits a given point*. In order to answer this question, we must make use of a density function. Let ΔA a finite area sensor that is smaller than the light field being measured. The spectral irradiance E is just the power per unit area $\frac{\Delta\Phi}{\Delta A}$ which is

$$E = \frac{\Delta q}{\Delta A \Delta t \Delta \lambda} \tag{2.1}$$

Thus the units of irradiance are $Jm^{-2}s^{-1}(nm)^{-1}$, the power per unit surface area.

Radiance

TODO: SHOW IMAGE: SOLID angle $WIKI : http : //en.wikipedia.org/wiki/Radiance$ $CGSlides2012 - 6.shading\ Book : Fundamentalsofcomputergraphics$

Although irradiance tells us how much light is arriving at a point, it tells us little about the direction that light comes from. To measure something similar to what we see with our eyes we need to be able to associate the quantity *how much light with a specific direction.*

Radiance is a measure of the quantity of radiation that passes through or is emitted from a surface and falls within a given solid angle in a specified direction. Think of it as the energy carried along a narrow beam of light. This means radiance characterizes the total emission of reflectance. It indicates how much of the power emitted by a reflecting surface will be received by an optical system looking at the surface from some given angle of view. Formally, this leads us to the following definition of radiance:

$$L(\omega) = \frac{d^2\Phi}{dAd\Omega cos(\theta)} \approx \frac{\Phi}{\Omega A cos(\theta)} \tag{2.2}$$

where L is the observed radiance in the unit energy per area per solid angle, which is $Wm^{-}2sr^{-}1$ in direction ω which has an angle θ between the surface normal and ω, Θ is the total flux or power emitted, θ is the angle between the surface normal and the specified direction, A is the area of the surface and Ω is the solid angle in the unit steradian subtended by the observation or measurement.

It is useful to distinguish between radiance incident at a point on a surface and exitant from that point. Terms for these concepts sometimes used in the graphics literature are surface radiance L_r for the radiance *reflected* from a surface and field radiance L_i for the radiance *incident* at a surface.

BRDF

The bidirectional reflectance distribution function, in short BRDF, denoted as $f_r(\omega_i, \omega_r)$ is a four dimensional function that defines *how light is reflected at an opaque surface.* The function takes a negative directed incoming light direction, ω_i, and outgoing direction, ω_r as input argument. Both are defined with respect to the surface normal $\mathbf{n}$.Hence A BRDF returns the ratio of reflected radiance exiting along ω_r to the irradiance incident on the surface from direction ω_i, which is formally:

$$BRDF(\omega_i, \omega_r) = f_r(\omega_i, \omega_r) \tag{2.3}$$

$$= \frac{dL_r(\omega_r)}{dE_i(\omega_i)} \tag{2.4}$$

$$= \frac{dL_r(\omega_r)}{L_i(\omega_i)cos(\theta_i)d\omega_i} \tag{2.5}$$

L is the reflected radiance, E is the irradiance and θ_i is the angle between ω_i and the surface normal, $\mathbf{n}$. The index i indicates incident light, whereas the index r indicates reflected light.

Spectral Rendering
In Computer Graphics, spectral rendering is where a scene's light transport is modeled considering the whole span of wavelengths instead of R,G,B values (still relating on geometric optic, which ignore wave phase). The motivation is that real colors of the physical world are spectrum; trichromatic colors are only inherent to Human Visual System.

In Computer Graphics, when talking about Spectral Rendering, we are refering to use the whole span of wavelengths instead just using RGB values in order for rendering a scene's light transport. The motivation for using the whole wavelength spectrum is due to the fact that trichromatic colors are only inherent to human visual system and therefore many phenomenons are poorly represented just using trichromy.

Color spaces
In order to see how crucial the role human vision plays, we only have to look the the definition of color: *Color is the aspect of visual perception by which an observer may distinguish differences between two structure-free filds of view of the same size and shape such as may be caused by differences in the spectral composition of the radiant energy concerned in the oberservation.* - Wyszechki and Siles, 2000 mentioned in Computer Graphics Fundamentals Book.

Each color can be represented by three numbers, for instance defined by (X,Y,Z) tristimulus values. However, its primaries are imaginary, meanung that is is not possible to construct a device that has three light sources (all positive) that can reprodue all colors in the visible spectrum. A large number of (X,Y,Z) values do not even correspond to a phyisical color.

CIE 1931 RGB and CIE 1931 XYZ color spaces are the first mathematically defined color spaces. They were created by the International Commission on Illumination (CIE) in 1931.

The CIE's color matching functions $\overline{x}(\lambda)$, $\overline{y}(\lambda)$ and $\overline{z}(\lambda)$ are the numerical description of the chromatic response of the observer (described above). They can be thought of as the spectral sensitivity curves of three linear light detectors yielding the CIE tristimulus values X, Y and Z. Collectively, these three functions are known as the CIE standard observer.[9]

The tristimulus values for a color with a spectral power distribution $I(\lambda)$, are given in terms of the standard observer by:

$$X = \int_{380}^{780} I(\lambda)\,\overline{x}(\lambda)\,d\lambda$$
$$Y = \int_{380}^{780} I(\lambda)\,\overline{y}(\lambda)\,d\lambda$$
$$Z = \int_{380}^{780} I(\lambda)\,\overline{z}(\lambda)\,d\lambda$$

where λ, is the wavelength of the equivalent monochromatic light (measured in nanometers).

It is not possible to build a display that corresponds to CIE XYZ, for this reasons it is necessary to design other color spaces, which are phyiscal realizable, offers efficient encoding, are perceptual uniform and have an intuitive color specification.

There are simple conversions between XYZ color space to any other color space defined, as linear transfromations.

2.1.3 Signal Processing Basics

A signal is a function that conveys information about the behavior or attributes of some phenomenon. In the physical world, any quantity exhibiting variation in time or variation in space (such as an image) is potentially a signal that might provide information on the status of a physical system, or convey a message between observers

Fourier Transformation
The Fourier-Transform is a mathematical tool which allows to transform a given function or rather a given signal from defined over a time- (or spatial-) domain into its corresponding frequency-domain.

Let f an measurable function over $\mathbb{R}^n$. Then, the continnous Fourier Transformation(**FT**), denoted as $\mathcal{F}\{f\}$ of f is defined as, ignoring all constant factors in the formula:

$$\mathcal{F}_{FT}\{f\}(w) = \int_{\mathbb{R}^n} f(x)e^{-iwt}dt \tag{2.6}$$

whereas its inverse transform is defined like the following which allows us to obtain back the original signal:

$$\mathcal{F}_{FT}^{-1}\{f\}(w) = \int_{\mathbb{R}} \mathcal{F}\{w\}e^{iwt}dt \tag{2.7}$$

An usual identity for w is the the so called angular with $w = \frac{2\pi}{T} = 2\pi v_f$ where T is the period, v_f the frequency.

By using Fourier Analysis, which is the approach to approximate any function by sums of simpler trigonometric functions, we gain the so called Discrete Time Fourier Transform (in short **DTFT**). The DTFT operates on a discrete function. Usually, such an input function is often created by digitally sampling a continnous function. The DTFT itself is operation on a discretized signal on a continnous, periodic frequency domain and looks like the following:

$$\mathcal{F}_{DTFT}\{f\}(w) = \sum_{-\infty}^{\infty} f(x)e^{-iwk} \tag{2.8}$$

We can further discretize the frequency domain and will get then the Discrete Fourier Transformation (in short **DFT**) of the input signal:

$$\mathcal{F}_{DFT}\{f\}(w) = \sum_{n=0}^{N-1} f(x)e^{-iw_nk} \tag{2.9}$$

Where the angular frequency w_n is defined like the following $w_n = \frac{2\pi n}{N}$ and N is the number of samples within an equidistant periode sampling.

Convolution
The convolution $f * g$ of two functions f, g: $\mathbb{R}^n \to \mathbb{C}$ is defined as:

$$(f * g)(t) = \int_{\mathbb{R}^n} f(t)g(t-x)dx \tag{2.10}$$

Note that the Fourier transform of the convolution of two functions is the product of their Fourier transforms. This is equivalent to the fact that Convolution in spatial domain is equivalent to multiplication in frequency domain. Therefore, the inverse Fourier transform of the product of two Fourier transforms is the convolution of the two inverse Fourier transforms

Taylor Series
Taylor series is a representation of a function as an infinite sum of terms that are calculated from the values of the function's derivatives at a single point.

The Taylor series $\mathcal{T}$ of a real or complex-valued function f(x) that is infinitely differentiable at a real or complex number a is the power series:

$$\mathcal{T}(f;a)(x) = \sum_{n=0}^{\infty} \frac{f^n(a)}{n!}(x-a)^n \tag{2.11}$$

2.2 Thesis Basis: J.Stam's Paper about Diffraction Shader

In his paper about Diffraction Shader, J. Stam derives a BRDF which is modeling the effect of diffraction for various analytical anisotropic reflexion models relying on the so called scalar wave theory of diffraction for which a wave is assumed to be a complex valued scalar. It's noteworthy, that Stam's BRDF formulation does not take into account the polarization of the light. Fortunately, light sources like sunlight and light bulbs are unpolarized.

A further assumption in Stam's Paper is, the emanated waves from the source are stationary, which implies the wave is a superposition of independent monochromatic waves. This implies that each wave is associated to a definite wavelangth lambda. However, sunlight once again fulfills this fact.

In our simulations we will always assume we have given a directional light source, i.e. sunlight. Hence, Stam's model can be used for our derivations.

For his derivations Stam uses the Kirchhoff integral (ADD REF TO WIKI), which is relating the reflected field to the incoming field. This equation is a formalization of Huygen's well-known principle that states that if one knows the wavefront at a given moment, the wave at a later time can be deduced by considering each point on the first wave as the source of a new disturbance. Mathematically speaking, once the field $\psi_1 = e^{ik\mathbf{x}\cdot\mathbf{ss}}$ on the surface is known, the field ψ_2 everywhere else away from the surface can be computed. More precisely, we want to compute the wave ψ_2 equal to the reflection of an incoming planar monochromatic wave $\psi_1 = e^{ik\omega_i * x}$ traveling in the direction ω_i from a surface S to the light source. Formally, this can be written as:

$$\psi_2(\omega_i, \omega_r) = \frac{ike^{iKR}}{4\pi R}(F(-\omega_i - \omega_r) - (-\omega_i + \omega_r)) \cdot I_1(\omega_i, \omega_r) \tag{2.12}$$

with

$$I_1(\omega_i, \omega_r) = \int_S \hat{\mathbf{n}} e^{ik(-\omega_i - \omega_r)\cdot \mathbf{s}} d\mathbf{s} \tag{2.13}$$

In applied optics, when dealing with scattered waves, one does use differential scattering cross-section rather than defining a BRDF which has the following identity:

$$\sigma^0 = 4\pi \lim_{R\to\infty} R^2 \frac{\langle |\psi_2|^2 \rangle}{\langle |\psi_1|^2 \rangle} \tag{2.14}$$

where R is the distance from the center of the patch to the receiving point x_p, $\hat{\mathbf{n}}$ is the normal of the surface at s and the vectors:

The relationship between the BRDF and the scattering cross section can be shown to be equal to

$$BRDF = \frac{1}{4\pi} \frac{1}{A} \frac{\sigma^0}{cos(\theta_i) cos(\theta_r)} \tag{2.15}$$

where θ_i and θ_r are the angles of incident and reflected directions on the surface with the surface normal n. See 2.3.

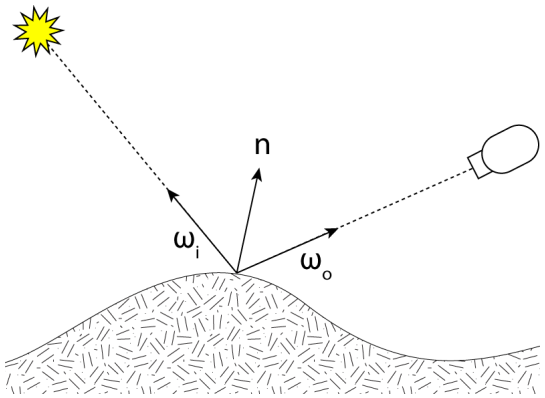

Abbildung 2.3: ω_i points toward the light source, ω_r points toward the camera, n is the surface normal

The components of vector resulting by the difference between these direction vectors: In order to simplify the calculations involved in his vectorized integral equations, Stam considers the components of vector

$$(u, v, w) = -\omega_i - \omega_r \tag{2.16}$$

explicitly and introduces the equation:

$$I(ku, kv) = \int_S \hat{\mathbf{n}} e^{ik(u,v,w)\cdot \mathbf{s}} d\mathbf{s} \tag{2.17}$$

which is a first simplification of 2.13. Note that the scalar w is the third component of 2.16 and can be written as $w = -(cos(\theta_i) + cos(\theta_r))$ using spherical coordinates. The scalar $k = \frac{2\pi}{\lambda}$ represent the wavenumber.

During his derivations, Stam provides a analytical representation for the Kirchhoff integral assuming that each surface point $s(x,y)$ can be parameterized by $(x,y,h(x,y))$ where h is the height at the position (x,y) on the given (x,y) surface plane. Using the tangent plane approximation for the parameterized surface and pluggin it into 2.17 he will end up with:

$$\mathbf{I}(ku,kv) = \int\int(-h_x(x,y),-h_y(x,y),1)e^{ikwh(x,y)}e^{ik(ux+vy)}dxdy \tag{2.18}$$

For further simplification Stam formulates auxilary function which depends on the provided heightfield:

$$p(x,y) = e^{iwkh(x,y)} \tag{2.19}$$

which will allow him to further simplifiy his equation 2.18 to:

$$\mathbf{I}(ku,kv) = \int\int\frac{1}{ikw}(-p_x,-p_y,ikwp)dxdy \tag{2.20}$$

where he used that $(-h_x(x,y),-h_y(x,y),1)e^{kwh(x,y)}$ is equal to $\frac{(-p_x,-p_y,ikwp)}{ikw}$ using the definition of the partial derivatives applied to the function 2.19.

Let $P(x,y)$ denote the Fourier Transform (FT) of $p(x,y)$. Then, the differentiation with respect to x respectively to y in the Fourier domain is equivalent to a multiplication of the Fourier transform by $-iku$ or $-ikv$ respectively. This leads him to the following simplification for 2.18:

$$\mathbf{I}(ku,kv) = \frac{1}{w}P(ku,kv)\cdot(u,v,w) \tag{2.21}$$

Let us consider the term $g = (F(-\omega_i-\omega_r)-(-\omega_i+\omega_r))$, which is a scalar factor of 2.12. The dot product with g and $(-\omega_i-\omega_r)$ is equal $2F(1+\omega_i\cdot\omega_r)$. Putting this finding and the identiy 2.21 into 2.12 he will end up with:

$$\psi_2(\omega_i,\omega_r) = \frac{ike^{iKR}}{4\pi R}\frac{2F(1+\omega_i\cdot\omega_r)}{w}P(ku,kv) \tag{2.22}$$

By using the identity 2.15, this will lead us to his main finding:

$$BRDF_\lambda(\omega_i,\omega_r) = \frac{k^2F^2G}{4\pi^2Aw^2}\langle|P(ku,kv)|^2\rangle \tag{2.23}$$

where G is the so called geometry term which is equal:

$$G = \frac{(1+\omega_i\cdot\omega_r)^2}{cos(\theta_i)cos(\theta_r)} \tag{2.24}$$

2.3 Derivations

2.3.1 BRDF formulation

Lets assume we have given an incoming light source with solid angle ω_i, θ_i is its angle of incidence, ω_r is the solid angle for the reflected light, λ wavelength, Ω is the hemisphre we of integration for the incomming light. Then, we are able to formulate a BRDF by using its definiton:

$$
\begin{aligned}
f_r(\omega_i, \omega_r) &= \frac{dL_r(\omega_r)}{L_i(\omega_i)cos(\theta_i)d\omega_i} \\
=> f_r(\omega_i, \omega_r)L_i(\omega_i)cos(\theta_i)d\omega_i &= dL_r(\omega_r) \\
=> \int_\Omega f_r(\omega_i, \omega_r)L_i(\omega_i)cos(\theta_i)d\omega_i &= \int_\Omega dL_r(\omega_r) \\
=> L_r(\omega_r) &= \int_\Omega f_r(\omega_i, \omega_r)L_i(\omega_i)cos(\theta_i)d\omega_i
\end{aligned}
$$

The last equation is the so called rendering equation. We assume further, that our incident light is a directional, unpolarized light source like sunlight and therefore its radiance is given as

$$L_\lambda(\omega) = I(\lambda)\delta(\omega - \omega_i) \tag{2.25}$$

where $I(\lambda)$ is the intensity of the relative spectral power for the wavelength λ. Since all light rays are parallel whenever we are provided by a directional light source and we can think of radiance as a measure of the light emitted from a particular surface location into a particular direction, above's radiance identity will follow immediately. By plugging this identity into our current rendering equation, we will get:

$$
\begin{aligned}
L_\lambda(w_r) &= \int_\Omega BRDF_\lambda(\omega_i, \omega_r)L_\lambda(\omega_i)cos(\theta_i)d\omega_i && (2.26) \\
&= BRDF_\lambda(\omega_i, \omega_r)I(\lambda)cos(\theta_i) && (2.27)
\end{aligned}
$$

where $L_\lambda(\omega_i)$ is the incomming radiance and $L_\lambda(\omega_r)$ is the radiance reflected by given surface Note that above's integral vanishes since $\delta(\omega - \omega_i)$ is only equal one if and only if $\omega = \omega_i$.

For the $BRDF(\omega_i, \omega_r)$ we are going to use Stam's main derivation (2.23) applying the fact that the wavenumber is equal $k = \frac{2\pi}{\lambda}$:

$$
\begin{aligned}
BRDF(\omega_i, \omega_r) &= \frac{k^2F^2G}{4\pi^2Aw^2}\langle|P(ku, kv)|^2\rangle \\
&= \frac{k^2F^2(1 + \omega_i \cdot \omega_r)^2}{cos(\theta_i)cos(\theta_r)4\pi^2Aw^2}\langle|P(ku, kv)|^2\rangle \\
&= \frac{4\pi^2F^2(1 + \omega_i \cdot \omega_r)^2}{cos(\theta_i)cos(\theta_r)4\pi^2A\lambda^2w^2}\langle|P(ku, kv)|^2\rangle \\
&= \frac{F(w_i, w_r)^2(1 + \omega_i \cdot \omega_r)^2}{cos(\theta_i)cos(\theta_r)A\lambda^2w^2}\langle|P(ku, kv)|^2\rangle
\end{aligned}
$$

going back to the definition of $(u, v, w) = -\omega_i - \omega_r$ and using spherical coordinates, we get for w the following identity $w = -\omega_i - \omega_r = -(\omega_i + \omega_r) = -(cos(\theta_i) + cos(\theta_r))$ and therefore w^2 is equal $(cos(\theta_i) + cos(\theta_r))^2$ This new fact will allow us to get even further:

$$
\begin{aligned}
L_\lambda(\omega_r) &= \frac{F(\omega_i,\omega_r)^2(1+\omega_i\cdot\omega_r)^2}{A\lambda^2 cos(\theta_i)cos(\theta_r)(cos(\theta_i)+cos(\theta_r))^2}\langle\left|P_{cont}(\frac{2\pi u}{\lambda},\frac{2\pi v}{\lambda})\right|^2\rangle cos(\theta_i)I(\lambda) \\
&= I(\lambda)\frac{F(\omega_i,\omega_r)^2(1+\omega_i\cdot\omega_r)^2}{\lambda^2 A(cos(\theta_i)+cos(\theta_r))^2 cos(\theta_r)}\langle\left|P_{cont}(\frac{2\pi u}{\lambda},\frac{2\pi v}{\lambda})\right|^2\rangle \\
&= I(\lambda)\frac{F(\omega_i,\omega_r)^2(1+\omega_i\cdot\omega_r)^2}{\lambda^2 A(cos(\theta_i)+cos(\theta_r))^2 cos(\theta_r)}\langle\left|T_0^2 P_{dtft}(\frac{2\pi u}{\lambda},\frac{2\pi v}{\lambda})\right|^2\rangle
\end{aligned}
$$

P_{cont} denotes the continuous inverse Fourier-Transform for the Taylor-Series of our heightfield representing the nano-scaled surface structure, i.e. $P(k,l) = \mathcal{F}^{-1}\{p\}(k,l)$ and P_{dtft} is the inverse Discrete Time Fourier Transform of $p(x,y) = e^{ikwh(x,y)}$. Furthermore T_0 the sampling distance for the discretization of $p(x,y)$ assuming equal and uniform sampling in both dimensions x,y.

2.3.2 Relative BRDF

In this section we are going to explain how to scale our BRDF formulation such that all of its possible output values are mapped into the range $[0,1]$. Such a relative BRDF formulation will ease our life for later rendering puposes since usually color values are within the range $[0,1]$, too. Furthermore, this will allow us to properly blend the resulting illumination caused by diffraction with a texture map.

Let us examine what $L_\lambda(\omega_r)$ will be for $\omega_r = \omega_0 := (0,0,*)$ i.e. specular reflection case, denoted as $L_\lambda^{spec}(\omega_0)$.

When we know the expression for $L_\lambda^{spec}(\omega_0)$ we would be able to compute the relative reflected radiance for our problem by simply dividing $L_\lambda(\omega_r)$ by $L_\lambda^{spec}(\omega_0)$, denoted as

$$
\rho_\lambda(\omega_i,\omega_r) = \frac{L_\lambda(\omega_r)}{L_\lambda^{spec}(\omega_0)} \tag{2.28}
$$

But first, let us derive the following expression:

$$
\begin{aligned}
L_\lambda^{spec}(\omega_0) &= I(\lambda)\frac{F(\omega_0,\omega_0)^2(1+\begin{pmatrix}0\\0\\1\end{pmatrix}\cdot\begin{pmatrix}0\\0\\1\end{pmatrix})^2}{\lambda^2 A(cos(0)+cos(0))^2 cos(0)}\langle\left|T_0^2 P_{dtft}(0,0)\right|^2\rangle \\
&= I(\lambda)\frac{F(\omega_0,\omega_0)^2(1+1)^2}{\lambda^2 A(1+1)^2 1}\left|T_0^2 N_{sample}\right|^2 \\
&= I(\lambda)\frac{F(\omega_0,\omega_0)^2}{\lambda^2 A}\left|T_0^2 N_{sample}\right|^2
\end{aligned}
$$

Where $N_{samples}$ is the number of samples of the DTFT.

Thus, we can plug our last derived expression into the definition for the relative reflectance radiance in the direction w_r and will get:

$$\begin{aligned}\rho_\lambda(\omega_i,\omega_r) &= \frac{L_\lambda(\omega_r)}{L_\lambda^{spec}(\omega_0)} \\ &= \frac{I(\lambda)\frac{F(\omega_i,\omega_r)^2(1+\omega_i\cdot\omega_r)^2}{\lambda^2 A(cos(\theta_i)+cos(\theta_r))^2 cos(\theta_r)}\langle\left|T_0^2 P_{dtft}(\frac{2\pi u}{\lambda},\frac{2\pi v}{\lambda})\right|^2\rangle}{I(\lambda)\frac{F(\omega_0,\omega_0)^2}{\lambda^2 A}\left|T_0^2 N_{sample}\right|^2} \\ &= \frac{F^2(\omega_i,\omega_r)(1+\omega_i\cdot\omega_r)^2}{F^2(\omega_0,\omega_0)(cos(\theta_i)+cos(\theta_r))^2 cos(\theta_r)}\langle\left|\frac{P_{dtft}(\frac{2\pi u}{\lambda},\frac{2\pi v}{\lambda})}{N_{samples}}\right|^2\rangle\end{aligned}$$

for simplification and a better overview, let us introduce the following expression, the so called gain-factor:

$$C(\omega_i,\omega_r) = \frac{F^2(\omega_i,\omega_r)(1+\omega_i\cdot\omega_r)^2}{F^2(\omega_0,\omega_0)(cos(\theta_i)+cos(\theta_r))^2 cos(\theta_r) N_{samples}^2} \tag{2.29}$$

Using this substitute, we will end up with the following expression for the relative reflectance radiance:

$$\rho_\lambda(\omega_i,\omega_r) = C(\omega_i,\omega_r)\langle\left|P_{dtft}(\frac{2\pi u}{\lambda},\frac{2\pi v}{\lambda})\right|^2\rangle \tag{2.30}$$

Using the previous definition for the relative reflectance radiance

$$\rho_\lambda(\omega_i,\omega_r) = \frac{L_\lambda(\omega_r)}{L_\lambda^{spec}(\omega_0)} \tag{2.31}$$

which we can rearrange to the expression

$$L_\lambda(\omega_r) = \rho_\lambda(\omega_i,\omega_r) L_\lambda^{spec}(\omega_0) \tag{2.32}$$

Let us choose $L_\lambda^{spec}(w_0) = S(\lambda)$ such that is has the same profile as the relative spectral power distribuation of CIE Standard Illuminant $D65$. Further, when integration over λ for a specular surface we should get CIE_{XYZ} values corresponding to the white point for $D65$ The corresponding tristimulus values using CIE colormatching functions for the CIE_{XYZ} values look like:

$$X = \int_\lambda L_\lambda(\omega_r)\overline{x}(\lambda)d\lambda \tag{2.33}$$

$$Y = \int_\lambda L_\lambda(\omega_r)\overline{y}(\lambda)d\lambda \tag{2.34}$$

$$Z = \int_\lambda L_\lambda(\omega_r)\overline{z}(\lambda)d\lambda \tag{2.35}$$

where $\overline{x}$, $\overline{y}$, $\overline{z}$ are the color matching functions

Using our last finding for $L_\lambda(\omega_r)$ with the definition for the tristimulus values we can actually derive an expression for computing the colors for our BRDF formula. Since X, Y, Z are defined similarly, it satisfies to derive an explicit expression for just one tristimulus term, for example X. The other two

will look the same, except the we have to replace all X with Y or Z respectively. Therefore, we get:

$$\begin{aligned}
X &= \int_\lambda L_\lambda(\omega_r)\overline{x}(\lambda)d\lambda \\
&= \int_\lambda \rho_\lambda(\omega_i,\omega_r)L_\lambda^{spec}(\omega_0)\overline{x}(\lambda)d\lambda \\
&= \int_\lambda \rho_\lambda(\omega_i,\omega_r)S(\lambda)\overline{x}(\lambda)d\lambda \\
&= \int_\lambda C(\omega_i,\omega_r)\langle\left|P_{dtft}(\frac{2\pi u}{\lambda},\frac{2\pi v}{\lambda})\right|^2\rangle S(\lambda)\overline{x}(\lambda)d\lambda \\
&= C(\omega_i,\omega_r)\int_\lambda \langle\left|P_{dtft}(\frac{2\pi u}{\lambda},\frac{2\pi v}{\lambda})\right|^2\rangle S(\lambda)\overline{x}(\lambda)d\lambda \\
&= C(\omega_i,\omega_r)\int_\lambda \langle\left|P_{dtft}(\frac{2\pi u}{\lambda},\frac{2\pi v}{\lambda})\right|^2\rangle S_x(\lambda)d\lambda
\end{aligned}$$

Where we used the definition $S_x(\lambda)\overline{x}(\lambda)$ in the last step.

2.3.3 Taylor approximation for BRDF

In this section, we will deliver an approximation for the inverse Fourier Tranformation of Stam's auxilary function p(x,y)s. This derivation will rely on the definition of Taylor Series expansion. Further, we will provide an error bound for our approximation approach for a given number of iterations. Last, we will extend our current BRDF formula by the findings derived within this section.

Given $p(x,y) = e^{ikwh(x,y)}$ form Stam's Paper where h(x,y) is a given heightfield. Let be y real or even complex value, and lets consider the power series for the the exponential function

$$e^t = 1 + t + \frac{t^2}{2!} + \frac{t^3}{3!} + ... = \sum_{n=0}^{\infty}\frac{t^n}{n!}$$

Let us define $t := t(x,y) = ikwh(x,y)$ where i is the imaginary number. For simplification, let us denote $h(x,y)$ as h. Then it follows by our previous stated identities:

$$\begin{aligned}
e^t &= 1 + (ikwh) + \frac{1}{2!}(ikwh)^2 + \frac{1}{3!}(ikwh)^3 + ... \\
&= \sum_{n=0}^{\infty}\frac{(ikwh)^n}{n!}.
\end{aligned}$$

Hence it holds $p(x,y) = \sum_{n=0}^{\infty}\frac{(ikwh(x,y))^n}{n!}$.

Let us now compute the Fourier Transformation of p(x,y) form above:

$$\begin{aligned}\mathcal{F}\{p\}(u,v) &= \mathcal{F}\left\{\sum_{n=0}^{\infty}\frac{(ikwh)^n}{n!}.\right\}(u,v)\\ &=^{\mathcal{F}\,lin\,Operator}\sum_{n=0}^{\infty}\mathcal{F}\left\{\frac{(ikwh)^n}{n!}\right\}(u,v)\\ &=\sum_{n=0}^{\infty}\frac{(ikw)^n}{n!}\mathcal{F}\{h^n\}(u,v)\end{aligned}$$

Hence it follows: $P(\alpha,\beta)=\sum_{n=0}^{\infty}\frac{(ikw)^n}{n!}\mathcal{F}\{h^n\}(\alpha,\beta)$ for which $\mathcal{F}_{FT}\{h^n\}(u,v)$.
Next we are going to look for an $N\in\mathbb{N}$ such that

$$\sum_{n=0}^{N}\frac{(ikwh)^n}{n!}\mathcal{F}\{h^n\}(\alpha,\beta)\approx P(\alpha,\beta)$$

is a good approximation. But first the following two facts have to be proven:

1. Show that there exist such an $N\in\mathbb{N}$s.t the approximation holds true.
2. Find a value for B s.t. this approximation is below a certain error bound, for example machine precision ϵ.

Proof Sketch of 1.

By the **ratio test** (see [**1**]) It is possible to show that the series $\sum_{n=0}^{N}\frac{(ikwh)^n}{n!}\mathcal{F}\{h^n\}(\alpha,\beta)$ converges absolutely:

Proof: Consider $\sum_{k=0}^{\infty}\frac{y^n}{n!}$ where $a_k=\frac{y^k}{k!}$. By applying the definition of the ratio test for this series it follows:

$$\forall y: limsup_{k\to\infty}|\frac{a_{k+1}}{a_k}| = limsup_{k\to\infty}\frac{y}{k+1}=0$$

Thus this series converges absolutely, no matter what value we will pick for y.

Part 2: Find such an N
Let $f(x)=e^x$. We can formulate its Taylor-Series, stated above. Let $P_n(x)$denote the n-th Taylor-Polinomial,

$$P_n(x)=\sum_{k=0}^{n}\frac{f^{(k)}(a)}{k!}(x-a)^k$$

where a is our developing point (here a is equal zero).

We can define the error of the n-th Taylor-Polinomial to be $E_n(x)=f(x)-P_n(x)$. the error of the n-th Taylor-Polinomial is difference between the value of the function and the Taylor polinomial This directly implies $|E_n(x)|=|f(x)-P_n(x)|$. By using the Lagrangien Error Bound it follows:

$$|E_n(x)|\leq\frac{M}{(n+1)!}|x-a|^{n+1}$$

with $a = 0$, where $\mathbf{M}$ is some value satisfying $|f^{(n+1)}(x)| \leq M$ on the interval $I = [a, x]$. Since we are interested in an upper bound of the error and since $\mathbf{a}$ is known, we can reformulate the interval as $I = [0, x_{max}]$, where

$$x_{max} = \|i\| k_{max} w_{max} h_{max}$$

We are interested in computing an error bound for $e^{ikwh(x,y)}$. Assuming the following parameters and facts used within Stam's Paper:

- Height of bump: 0.15micro meters
- Width of a bump: 0.5micro meters
- Length of a bump: 1micro meters
- $k = \frac{2\pi}{\lambda}$ is the wavenumber, $\lambda \in [\lambda_{min}, \lambda_{max}]$ and thus $k_{max} = \frac{2\pi}{\lambda_{min}}$. Since $(u, v, w) = -\omega_i - \omega_r$ and both are unit direction vectors, each component can have a value in range [-2, 2].
- for simplification, assume$[\lambda_{min}, \lambda_{max}] = [400nm, 700nm]$.

We get:

$$\begin{aligned} x_{max} &= \|i\| * k_{max} * w_{max} * h_{max} \\ &= k_{max} * w_{max} * h_{max} \\ &= 2 * (\frac{2\pi}{4 * 10^{-7} m}) * 1.5 * 10^{-7} \\ &= 1.5\pi \end{aligned}$$

and it follows for our intervall $I = [0, 1.5\pi]$.

Next we are going to find the value for M. Since the exponential function is monotonically growing (on the interval I) and the derivative of the **exp** function is the exp function itself, we can find such an M:

$$\begin{aligned} M &= e^{x_{max}} \\ &= exp(1.5\pi) \end{aligned}$$

and $|f^{(n+1)}(x)| \leq M$ holds. With

$$\begin{aligned} |E_n(x_{max})| &\leq \frac{M}{(n+1)!} |x_{max} - a|^{n+1} \\ &= \frac{exp(1.5\pi) * (1.5\pi)^{n+1}}{(n+1)!} \end{aligned}$$

we now can find a value of n for a given bound, i.e. we can find an value of $N \in \mathbb{N}$ s.t. $\frac{exp(1.5\pi) * (1.5\pi)^{N+1}}{(N+1)!} \leq \epsilon$. With Octave/Matlab we can see:

- if N=20 then $\epsilon \approx 2.9950 * 10^{-4}$
- if N=25 then $\epsilon \approx 8.8150 * 10^{-8}$

- if N=30 then $\epsilon \approx 1.0050 * 10^{-11}$

With this approach we have that $\sum_{n=0}^{25} \frac{(ikwh)^n}{n!} \mathcal{F}\{h^n\}(\alpha, \beta)$ is an approximation of $P(u,v)$ with error $\epsilon \approx 8.8150 * 10^{-8}$. This means we can precompute 25 Fourier Transformations in order to approximate P(u,v) having an error $\epsilon \approx 8.8150 * 10^{-8}$.

Using now our approximation for $P_{dtft} = \mathcal{F}^{-1}\{p\}(u,v)$ for the tristumulus value X, we will get:

$$\begin{aligned} X &= C(w_i, w_r) \int_\lambda \langle \left| P_{dtft}(\frac{2\pi u}{\lambda}, \frac{2\pi v}{\lambda}) \right|^2 \rangle S_x(\lambda) d\lambda \\ &= C(w_i, w_r) \int_\lambda \left| \sum_{n=0}^{N} \frac{(wk)^n}{n!} \mathcal{F}^{-1}\{i^n h^n\}(\frac{2\pi u}{\lambda}, \frac{2\pi v}{\lambda}) \right|^2 S_x(\lambda) d\lambda \end{aligned}$$

2.3.4 Sampling: Gaussian Window

Practically, we cannot compute the DTFT numerically due to finite computer arithmetic, since w is a continuous function for the DTFT. The DFT of a discrete heightfield patch is equivalent to the DTFT of an infinitely periodic function consisting of replicas of the same discrete patch. By windowing with a window function that is zero outside the central replica, the convolution of either the DFT or the DTFT of heightfield with the fourier transfrom of the window becomes equivalent.

Let $window_g$ denote the gaussian window with $4\sigma_s$ μm where $\sigma_f = \frac{1}{2\pi\sigma_s}$ let us further substitute $\mathbf{t}(\mathbf{x}, \mathbf{y}) = i^n h(x,y)^n$

$$\mathcal{F}^{-1}_{dtft}\{\mathbf{t}\}(u,v) = \mathcal{F}^{-1}_{fft}\{\mathbf{t}\}(u,v) window_g(\sigma_f) \tag{2.36}$$

Therefore we can deduce the following expression from this:

$$\begin{aligned} \mathcal{F}^{-1}_{dtft}\{\mathbf{t}\}(u,v) &= \int_{-\infty}^{\infty} \int_{-\infty}^{\infty} F^{-1}_{fft}\{\mathbf{t}\}(w_u, w_v) \phi(u - w_u, v - w_v) dw_u dw_v \\ &= \int_{-\infty}^{\infty} \int_{-\infty}^{\infty} \sum_i \sum_j F^{-1}_{fft}\{\mathbf{t}\}(w_u, w_v) \\ &\qquad \delta(w_u - w_i, w_v - w_j) \phi(u - w_u, v - w_v) dw_u dw_v \\ &= \sum_i \sum_j \int_{-\infty}^{\infty} \int_{-\infty}^{\infty} F^{-1}_{fft}\{\mathbf{t}\}(w_u, w_v) \\ &\qquad \delta(w_u - w_i, w_v - w_j) \phi(u - w_u, v - w_v) dw_u dw_v \\ &= \sum_i \sum_j F^{-1}_{fft}\{\mathbf{t}\}(w_u, w_v) \phi(u - w_u, v - w_v) \end{aligned}$$

where

$$\phi(x,y) = \pi e^{-\frac{x^2+y^2}{2\sigma_f^2}} \tag{2.37}$$

2.3.5 Final Expression

As the last step of our series of derivations, we plug all our findings together to one big equation in order to compute the color for each pixel on our mesh in the CIE_XYZ colorspace:

For a given heigh-field $h(x,y)$, representing a small patch of the nano-structure of our surface, the resulting CIE_{XYZ} caused by the effect of diffraction can be computed like the following:

Let $P(u,v,\lambda) = F_{fft}^{-1}\{i^n h^n\}(\frac{2\pi u}{\lambda}, \frac{2\pi v}{\lambda})$

$$\begin{pmatrix} X \\ X \\ Z \end{pmatrix} = C(\omega_i, \omega_r) \int_\lambda \sum_{n=0}^{N} \frac{(wk)^n}{n!} \sum_{(r,s)\in\mathcal{N}_1(u,v)} |P_\lambda(u-w_r, v-w_s)|^2 \phi(u-w_r, v-w_s) \begin{pmatrix} S_x(\lambda) \\ S_y(\lambda) \\ S_z(\lambda) \end{pmatrix} d\lambda \tag{2.38}$$

where $\phi(x,y) = \pi e^{-\frac{x^2+y^2}{2\sigma_f^2}}$ is the gaussian window. where w_s and w_r are ... explain them

2.4 Alternative Approach

REASON FOR WHICH CASE THIS CAN BE USED, ADD AN IMAGE OF BOXFUNCTION The approach introduced within this section is an alternative to the gaussian window approach. Let us consider the so called 1-dimensional Box-function with length T which is defined as the following:

$$Box(x) = \begin{cases} 1 & \text{if } x \leq T \\ 0 & \text{if } else \end{cases}$$

We assume, that our given heighfield can be represented as a 2-dimensional box-function. Note that we can use any explicit given constrainted 2-dimensional function and will get some identities like we get from the box-function.

Further we are assuming that we can model the overall surface be assuming this heighfield being distributed in a periodic manor. Therfore, the whole surface can be represented like this $f(x) = \sum_{n=0}^{N} Box(x+nT_1, y+mT_2)$ assuming the given heighfield has the dimensions T_1 by T_2. But let us first consider the 1-dimensional Box-function case before deriving an identity for the Fourier transform of our 2-dimensional Box-function, i.e. the fourier transform of our heighfield.

Note: A function f periodic with periode T means: $\forall x \in \mathcal{R} : Box(x) = Box(x+T)$

A so called bump can be represented by our 1-dimensional Box-function. We assume periodicity which is equaivalent to: $f(x) = \sum_{n=0}^{N} Box(x+nT)$

We are insterested in the 1-dimensional inverse Fourier transform of the 1-dimensional Box-function:

$$\begin{aligned}\mathcal{F}^{-1}\{f\}(w) &= \int f(x)e^{iwx}dx \\ &= \int_{-\infty}^{\infty} \sum_{n=0}^{N} Box(x+nT)e^{iwx}dx \\ &= \sum_{n=0}^{N} \int_{-\infty}^{\infty} Box(x+nT)e^{iwx}dx\end{aligned}$$

Next, apply the following substituation $x + nT = y$ which will lead us to:

$$\begin{aligned}x &= y - nT \\ dx &= dy\end{aligned}$$

Plugging this substituation back to the equation from above we will get

$$\begin{aligned}\mathcal{F}^{-1}\{f\}(w) &= \int f(x)e^{iwx}dx \\ &= \sum_{n=0}^{N} \int_{-\infty}^{\infty} Box(y)e^{iw(y-nT)}dy \\ &= \sum_{n=0}^{N} e^{-iwnT} \int_{-\infty}^{\infty} Box(y)e^{iwy}dy \\ &= \sum_{n=0}^{N} e^{-iwnT}\mathcal{F}\{f\}(w) \\ &= \mathcal{F}^{-1}\{f\}(w) \sum_{n=0}^{N} e^{-iwnT}\end{aligned}$$

We used the fact that the term e^{-iwnT} is a constant when integrating along dy and the identity for the inverse Fourier transform of the Box function. Next, let us consider $\sum_{n=0}^{N} e^{-uwnT}$ further:

$$\begin{aligned}\sum_{n=0}^{N} e^{-uwnT} &= \sum_{n=0}^{N} (e^{-uwT})^n \\ &= \frac{1 - e^{iwT(N+1)}}{1 - e^{-iwT}}\end{aligned}$$

We recognize the geometric series identity for the left-handside of this equation. Since our series is bounded we can derive our right-handside.

Since e^{-ix} is a complex number and every complex number can be written in its polar form, i.e. $e^{-ix} = cos(x) + isin(x)$ we can go even further, using the trigonometric idententities that $cos(-x) = cos(x)$ and $sin(-x) = -sin(x)$:

$$\frac{1 - e^{iwT(N+1)}}{1 - e^{-iwT}} = \frac{1 - cos(wT(N+1)) + isin(wT(N+1))}{1 - cos(wT) + isin(wT)}$$

Which is still a complex number $(p+iq)$. Every complex number can be written as a fraction of two complex numbers. This means that the complex number $(p+iq)$ can be written as $(p+iq) = \frac{(a+ib)}{(c+id)}$ for any $(a+ib), (c+id) \neq 0$. For our case, let us use the follwoing substituations:

$$a := 1 - cos(wT(N+1)) \qquad b = sin(wT(N+1)) \tag{2.39}$$
$$c = 1 - cos(wT) \qquad d = sin(wT) \tag{2.40}$$

hence it follows $\frac{1-e^{iwT(N+1)}}{1-e^{-iwT}} = \frac{(a+ib)}{(c+id)}$. By rearanging the terms it follows $(a+ib) = (c+id)(p+iq)$ and multiplying the right handside out we get the follwing system of equations:

$$(cp - dq) = a \tag{2.41}$$
$$(dp + cq) = b \tag{2.42}$$

Which gives lead us we some further math (trick: mult first eq. by c and 2nd by d, then adding them together. using distributivity and we have the identity for p for example, similar for q) to

$$p = \frac{(ac+bd)}{c^2+d^2} \tag{2.43}$$
$$q = \frac{(bc+ad)}{c^2+d^2} \tag{2.44}$$

Putting our substituation for a, b, c, d back into the current representatio for p and q and using some trigonometric identites, this we then get:

$$p = \frac{1}{2} + \frac{1}{2}\left(\frac{cos(wTN) - cos(wT(N+1))}{1 - cos(wT)}\right) \tag{2.45}$$
$$q = \frac{sin(wT(N+1)) - sin(wTN) - sin(wT)}{2(1 - cos(wT))} \tag{2.46}$$

Since we have seen, that $\sum_{n=0}^{N} e^{-uwnT}$ is a complex number and can be written as $(p+iq)$ and we know now the explicit identity for those p and q we get for the 1-dimensional Fourier transform of the 1-dimensional Box-function the following final identity:

$$\begin{aligned}\mathcal{F}^{-1}\{f\}(w) &= \mathcal{F}^{-1}\{f\}(w) \sum_{n=0}^{N} e^{-iwnT} \\ &= (p+iq)\mathcal{F}^{-1}\{Box\}(w)\end{aligned}$$

In oder to derive next a identity for the Fourier transform for our 2-dim heighfield, we can proceed similarly, the only fact which changes is, that we are now in a 2-dimensional domain, i.e. we are about to compute a two-dimensional

Fourier transform: Let us again us again a Box-function, this time a 2-dimensional Box-function $Box(x,y)$ just for the sake of convenience.

$$\begin{aligned}
\mathcal{F}^{-1}\{f\}(w_1,w_2) &= \int_{-\infty}^{\infty}\int_{-\infty}^{\infty}\sum_{n_2=0}^{N_1}\sum_{n_2=0}^{N_2} Box(x_1+n_1T_1, x_2+n_2T_2)e^{iw(x_1+x_2)}dx_1dx_2 \\
&= \int_{-\infty}^{\infty}\int_{-\infty}^{\infty}\sum_{n_2=0}^{N_1}\sum_{n_2=0}^{N_2} Box(y_1,y_2)e^{iw((y_1-n_1T_1)+(y_2+n_2T_2))}dx_1dx_2 \\
&= \sum_{n_2=0}^{N_1}\sum_{n_2=0}^{N_2}\int_{-\infty}^{\infty}\int_{-\infty}^{\infty} Box(y_1,y_2)e^{iw(y_1+y_2)}e^{-iw(n_1T_1+n_2T_2)}dy_1dy_2 \\
&= \sum_{n_2=0}^{N_1}\sum_{n_2=0}^{N_2} e^{-iw(n_1T_1+n_2T_2)}\int_{-\infty}^{\infty}\int_{-\infty}^{\infty} Box(y_1,y_2)e^{iw(y_1+y_2)}dy_1dy_2 \\
&= \left(\sum_{n_2=0}^{N_1}\sum_{n_2=0}^{N_2} e^{-iw(n_1T_1+n_2T_2)}\right)\mathcal{F}^{-1}\{Box\}(w_1,w_2) \\
&= \left(\sum_{n_2=0}^{N_1} e^{-iwn_1T_1}\right)\left(\sum_{n_2=0}^{N_2} e^{-iwn_2T_2}\right)\mathcal{F}^{-1}\{Box\}(w_1,w_2) \\
&= (p_1+iq_1)(p_2+iq_2)\mathcal{F}^{-1}\{Box\}(w_1,w_2) \\
&= ((p_1p_2-q_1q_2)+i(p_1p_2+q_1q_2))\mathcal{F}^{-1}\{Box\}(w_1,w_2) \\
&= (p+iq)\mathcal{F}^{-1}\{Box\}(w_1,w_2)
\end{aligned}$$

Where we define $p := (p_1p_2 - q_1q_2)$ and $q := (p_1p_2 + q_1q_2)$. For this identity we used green's integration rule which allowed us to split the double integral to the product of two single integrations. Also, we used the definition of the 2-dimensional inverse Fourer transform of the Box-function. We applied the same substituation like we did in for the 1 dimensional case, but this time twice, once for each variable seperately. The last step, substituting with p and q will be useful later in the implementation. The insight should be, that the product of two complex numbers is again a complex number. We will have to compute the absolute value of $\mathcal{F}^{-1}\{f\}(w_1,w_2)$ which will then be equal $(p^2+q^2)^{\frac{1}{2}}\left|\mathcal{F}^{-1}\{Box\}(w_1,w_2)\right|$

Kapitel 3

Implementation

In computergraphics, we are interested in synthesizing 2d images from a given scene containing our 3d geometries by using so called shader programs. This process is denoted as rendering. The purpose of shader programs, which are executed directly on the GPU hardware device, is to compute the colorization and illumination of the objects living in our scene. All these computations happen in several stages and depend on the provided scene-input parameters like the camera, light sources, objects material constants and the desired rendering effect one is interested in to model. The shader stages are implemented sequencially as small little programs, the so called vertex-, geometry- and fragment-shaders. Those stages are applied within the rendering pipeline sequencially.

Our shaders which we use are written in a high-level language called GLSL, the OpengGL Shading Language. The decission for using OpenGL has been made since my underlying framework, which is responsible for the precomputation of all scene date, is based on another framework, written in Java using JOGL in oder to communicate with the GPU and is also responsible to precompute all the relevant scene data. This framework, the so called jrtr framework, has been developed as an exercise during the class computer graphics held by M. Zwicker which I attended in autumn 2012. The framework itself has been used and further extended during this thesis quite a lot. All necessary input data required for our java framework in order to perform the shading is precomputed by using Matlab. This is basically addressing all the required precomputations for the provided heigh-fields, refering to computation of the inverse two dimensional Fourier transformations which are further explained within this chapter. The Matlab scripts themself rely on the provided snake nano-scaled sheds images, taken by AFM.

It's noteworthy that all the vertices are processed within the vertex-shader, whereas the fragement shader's responsibility is to perfrom pixelwise rendering, using the input from the vertex shader. Just remember, fragements are determined by a triple of vertices. hence each pixel has assigned a trilinear interpolated value of all input parameters of its spanning vertices. Usually, all necessary transformations are applied vertex-wise, considering the vertex-shader as the precomputation stage for the later rendering within the rendering pipeline, in the fragment-shader. In the geometry shader, new vertices around a considered vertex can be created. this is useful for debugging - displaying normals graphically for example.

In this part of thesis we are going to explain how we render our BRDF formulation derived in the last section in practice. all the necessary computations in order to simulate the effect of diffraction are performed within a fragment shader. This implies that we are modeling the effect of diffraction pixelwise and hence the overall modeling quality and computional pace depends on rendering window's resolution.

By the end of this chapter we will have seen how our how our render works, what we have to precompute and how our shaders work.

3.1 Precomputations in Matlab

Our first task is to precompute the inverse two dimensional discrete Fourier Transformations of a given snake shed patch of interest taken by AFM. For that purpose we have written a small Matlab script which offers a huge collection of mathematically, nummerically fast and stable algorithms. Our Matlab script reads a given image, which is representing a nano-scaled heightfield, and computes its inverse two dimensional DFT by using Matlab's internel inverse fast Fourier Transformation function, denoted by $ifft2$. Note that we only require once color channel of the input image since the input image is representing an heightfield, encoded by just one color. Basically, we are interested in computing the $ifft2$ for different powers of the input image since our taylor series approximation for the overall computation relies on this. Keep in mind that taking the Fourier Transformation of an arbitrary function will result in a complex valued output which implies that we will get a complex value for each pixel of our input image. Therefore, for each input image we get as many output images, representing the two dimensional inverse Fourier Transformation, as the minimal amount of taylor terms required for a well-enough approximation. In order to store our output images, we have to use 2 color channels instead just one like it was for the given input image. As an optimization step, we do not directly store images, rather we output binary files which contain all RGB values for each pixel in a row first, column last format. This allows us to have much higher precision for the output values and also it does not waste any color channels. Note that we have scaled each pixel value in a range between 0 and 1. Therefore, we have to remember store four scaling factors for each output image as well, which are the real and imaginary minimum and maximum values. Later, using linear interpolation within the shader, we will get back the image's original values.

Algorithm 3.1 Precomputation: Fourier images

```
% maxH:     A floating-point number specifying
%           the value of maximum height of the
%           height-field in MICRONS, where the
%           minimum-height is zero.
%
% dH:       A floating-point number specifying
%           the resolution (pixel-size) of the
%           'discrete' height-field in MICRONS.
%           It must less than 0.1 MICRONS to
%           ensure proper response for
%           visible-range of light spectrum.
%
% termCnt: An integer specifying the number of
%           Taylor series terms to use.

function []= ComputeFFTImages(maxH, dh, termCnt)
dH = dh*1E-6;
% load patch into patchImg
patchImg = patchImg.*maxH;
% perform imrotate(patchImg, angle)
for t = 0 : termCnt
  patchFFT = power(1j*patchImg, t);
  fftTerm{t+1} = fftshift(ifft2(patchFFT));

  imOut(:,:,1)  = real(fftTerm{t+1});
  imOut(:,:,2)  = imag(fftTerm{t+1});
  imOut(:,:,3)  = 0.5;

  % perform imrotate(imOut, -angle)
  % find real and imaginary extrema of
  % write imOut, extrema, dH, into files.
end
```

The command fftshift rearranges the output of the ifft2 by moving the zero frequency component to the centre of the image. This is useful for visualizing a Fourier Transform with zero frequency components in the middle of the spectrum.

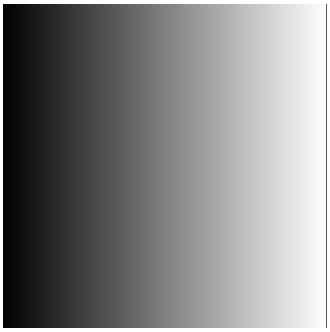

(a) Blaze Patch

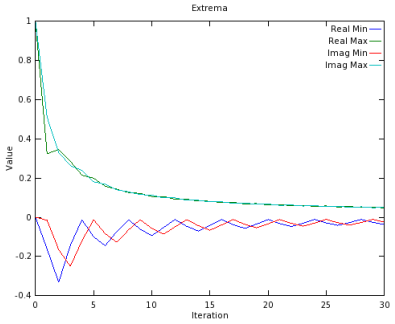

(b) Extrema Plot

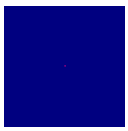

(c) ImRe0

(d) ImRe1

(e) ImRe4

(f) ImRe10

(g) ImRe20

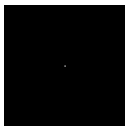

(h) Re0

(i) Re1

(j) Re4

(k) Re10

(l) Re20

(m) Im0

(n) Im1

(o) Im4

(p) Im10

(q) Im20

Abbildung 3.1: Blaze

TODO: say something about output?

3.2 Our Java Renderer

In autumn 2012, during the semester I have attented the class computer graphics held by M. Zwicker. During the whole class we have developed a so called real time renderer program written in java as a series of homework assignments in order to be admitted to the final exam. The architecture of the program is divided into two parts: a rendering engine, the so called jrtr (java real time renderer) and an application program, denoted as scene.

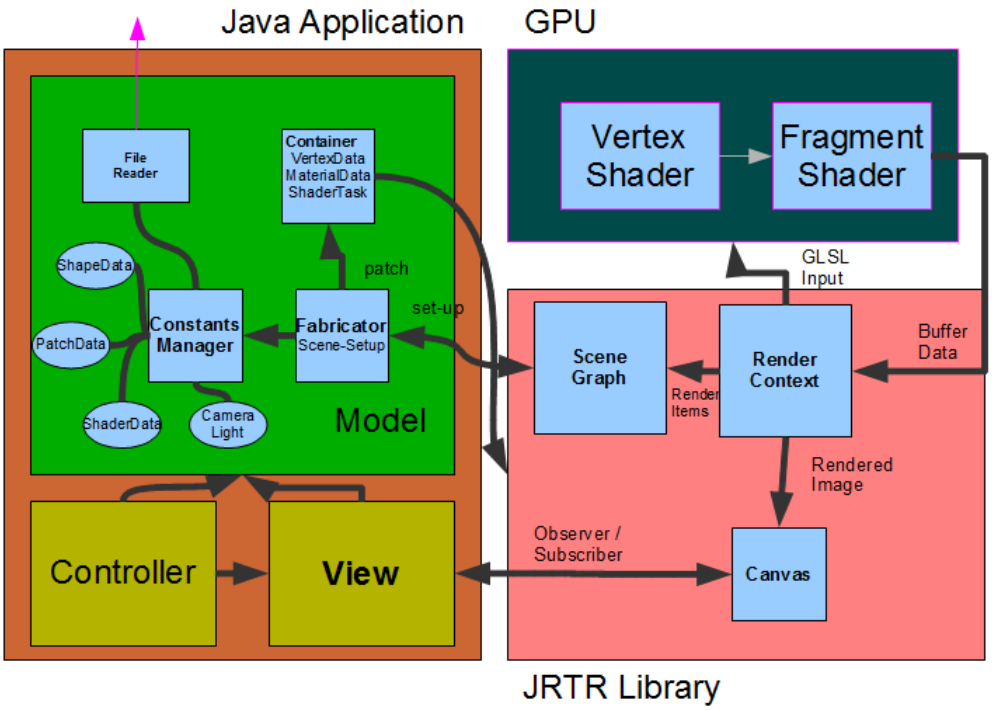

Abbildung 3.2: Renderer Architecture

the scene application program task was basically to define the whole scene we is going to be rendered within jrtr later. A scene consists of the setup of the world camera, definitions of light source, frustum, geometries which live in our scene and their material constants. Such materials are textures for example. All those scene attributes are managed within jrtr. In the application program, there only happens their definition. The minimal definition of a geometry is given by its wireframe mesh. This is a datastructures consisting of vertices each stored as a triple of xyz positions in an float array and triangles each defined by a triple of vertex-indices which form a fragment each stored in an integer array. It is possible to assing additional geoemtry data like a color for each vertex, normals and texture coordinates. All whole scene is stored within container data-structures, defined and managed within jrtr, like a scene graph, which contains all geometries and their transformations in a tree like structured hierarchy. The geometries themself are stored within an container, containing all vertex attributes and the material constants. The jrtr rendering engine uses a low-level API, called openGL in order to communicate with the grpahcis processor unit (GPU). Within jrtr, the whole resource-management for the rendering pipeline place, i.e. all required low-level buffers are allocated, flushed and assigned by the scene data attributes. jrtr also offers also the possibility to assign arbitrary shaders.

3.2.1 Scene

what is done here reworked such that it is mvc-architecute based user-interaction: handlers in GUI. which geometries are defined what material constants are defined: mention fabricators: light, camera, materials,... file readers: monkey

3.2.2 jrtr Framework

shader tasks assign all shader inputs: like t0 and so on load fourier images and assign to buffers snapshot functionality shaders: diffraction shader

3.3 GLSL Diffraction Shader

TODO: start using the final findings from chapter 2 and substitute

3.3.1 Vertex Shader

The first computional stage within our rendering pipeline is computing all necessary per vertex data. Those computations are preformed in the vertex shader. In our case, we compute for any vertex of our current geometry the direction vectors $k1$ and $k2$ described like previousely in the tangent space. Initially all input data lives in its own space. Hence, we first have to transfrom all input data into the same space in order to use it for later computations within the fragment shader. We are going to transform k1 and k2 into the so called tangent space which. Furthermore, we have also to realign our local coordinate system. This is why there is an rodrigues rotation also involved. In order to avoid scaling issues and since we are only interested in the direction of the vectors k1 and k2, we have to normalize them, too. Last, we also output the position of the current vertex transfomed into the projective camera space.

explain cop_w modelM other shader assigned inputs

Algorithm 3.2 Vertex diffraction shader

foreach *Vertex* $v \in$ *Shape* **do**
$vec3N = normalize(modelM * vec4(normal, 0.0)).xyz$
$vec3T = normalize(modelM * vec4(tangent, 0.0)).xyz$
$T = rotateRodrigues(T, N, phi)$
$vec3B = normalize(cross(N, T))$
$vec3Pos = ((cop_w - position)).xyz$
$vec4lightDir = (directionArray[0])$
$lightDir = normalize(lightDir)$
$l = projectVectorOnTo(lightDir, TangentSpace)$
$p = projectVectorOnTo(Pos, TangentSpace)$
$normalize(l); normalize(p)$
$gl_Position = projection * modelview * position$
end for

3.3.2 Fragment Shader

The purpose of a fragment shader is to render per fragment. A fragment is spanned by three vertices of a given mesh. For each pixel within all the output from the vertex shaders of its corresponding vertices is then trilinearly interpolated, depending on the pixel's position within the fragment, and passed into its fragment shader program. Furthermore, there can be additional input be assigned which is not directly interpolated from the output of vertex shader programs. Our fragment shader just relies on k1 and k2 from its vertex shaders for the computation of the effect of diffraction. There are some values preliminarily assigned to our fragment shader during the opgenGL setup within our java program, like all references to the image buffers, containing the Fourier Transformations, the number of taylor step approximations, the minimal and maximal wavelength, other lookup values like the scaling factors, a reference to a lookup table containing the CIE_{XYZ} color weights for our wavelength domain and other scaling constants.

Our shader performs an on-the-fly numerical integration for the integral in the derivation using trapeziodal rule with uniform discretization of the λ dimension at a resolution of 5nm. To compute $F_{dtft}\{p\}$ terms the shader uses he precomputed DFTs for the Taylor series terms given in the derivation. The Gaussian window approach is performed for each discrete λ value using a window large enough to span $4\sigma_f$ in both dimensions. For computing DFT tables we generally use nanostructure hieghtfields that span at least $65\mu m^2$ and are sampled with resolution of at least 100nm. This ensures that the spectral response encompasses al the wavelengths in the visible spectrum, i.e. from 380nm to 780nm. Note that this shader is not very fast in hardly can be denoted being interactive.

mention we uniform discretize λ for a given (u,v) which implies compressing sampled frequencies to the region near to the origin (of their frequency domain). For natural structures in nano-scale, most of their spectral energy lies at lower spatial frequencies which maps closer to region $(u, v) = (0, 0)$ than higher frequencies. This is why We have chosen to sample (u,v) space non-linearly. We use 30 Taylor-terms for our approximation approach which has an error below Y, proven in the previous derivation chapter.

Algorithm 3.3 Fragment diffraction shader

1: **foreach** *Pixel* $p \in$ *Fragment* **do**
2: **INIT** $BRDF_{XYZ}, BRDF_{RGB}$ **TO** $vec4(0.0)$
3: $(u, v, w) = \hat{\mathbf{k_1}} - \hat{\mathbf{k_2}}$
4: **for** $(\lambda = \lambda_{min}; \lambda \leq \lambda_{max}; \lambda = \lambda + \lambda_{step})$ **do**
5: $xyzWeights = getClrMatchingFnWeights(\lambda)$
6: $lookupCoord = getLookupCoord(u, v, \lambda)$
7: **INIT** P **TO** $vec2(0.0)$
8: $k = \frac{2\pi}{\lambda}$
9: **for** $(n = 0$ **TO** $MAXTAYLORTERMS)$ **do**
10: $taylorScaleF = \frac{(kw)^n}{n!}$
11: **INIT** F_{fft} **TO** $vec2(0.0)$
12: $anchorX = int(floor(center.x + lookupCoord.x * fftImWidth)$
13: $anchorY = int(floor(center.y + lookupCoord.y * fftImHeight)$
14: **for** $(i = (anchorX - winW)$ **TO** $(anchorX + winW + 1))$ **do**
15: **for** $(j = (anchorY - winW)$ **TO** $(anchorY + winW + 1))$ **do**
16: $dist = getDistVecFromOriginFor(i, j)$
17: $position = getLocalLookUp(i, j, n)$
18: $fftVal = getRescaledFourierTextureValueAt(position)$
19: $fftVal *= getGaussWeightAtDistance(dist)$
20: $F_{fft} += fftVal$
21: **end for**
22: **end for**
23: $P += taylorScaleF * F_{fft}$
24: **end for**
25: $xyzPixelColor += dot(vec3(|P|^2), xyzWeights)$
26: **end for**
27: $BRDF_{XYZ} = xyzPixelColor * C(\hat{\mathbf{k_1}}, \hat{\mathbf{k_2}}) * shadowF$
28: $BRDF_{RGB}.xyz = D_{65} * M_{XYZ-RGB} * BRDF_{XYZ}.xyz$
29: $BRDF_{RGB} = gammaCorrect(BRDF_{RGB})$
30: **end for**

From line 4 to 26:
Within this loop happens the uniform sampling along lambda space. At line 5: $getClrMatchingFnWeights(\lambda)$ computes the color weights for the current wavelength by bilinear interpolation from the two closest given CIE_{XYZ} color weights for our current wavelength λ. At line 6: $getLookupCoord(u, v, \lambda)$ computes the current coordinate for the texture lookup in our precomputed ifft2 images.

From line 9 to 24:
Within this loop happens the taylor series approximation till a predefined upper bound, denoted as $MAXTAYLORTERMS$. Basically, the spectral response is approximated for our current (u, v, λ). Furthermore, neighborhood-bounds for the upcoming gaussian windowing-sampling-approach are computed, denoted as anchorX and anchorY.

From line 14 to 22:
In this most inner loop the convolution of the gaussian window with the inver-

se FFT of the patch is pixelwise performed. *getGaussWeightAtDistance*(*dist*) computes (2.37) from the distance between the center of the FFT image with the current position in the neighborhood in texture space. *getRescaledFourierTextureValueAt*(*position*) rescales the current computed value by the precomputed extrema values since all image values are scaled between 0 and 1. At line 27 $C(\hat{\mathbf{k_1}}, \hat{\mathbf{k_2}})$ is multiplied in front of the current computed pixel-color. This terms was introduced in the derivation chapter and is the product of equation (2.29)

The C term includes is the gain factor 2.29. We compute this by using the so called Schlick approximation $A.1$ using an reactive index at 1.5 since this is close to the measured value from snake sheds.

Our BRDF values are scaled by s shadowing function as described in (SEE REFERENCES - PAPER), since most of the grooves in the snake skin nano-structures would from a V-cavity along the plane for a wave front with their top-edges at almost the same height.

SHOW GRAPH for this fact: (lambda, k=f(lambda)), where $k = \frac{2pi}{\lambda}$, $f = \frac{c}{\lambda}$

3.4 Technical details

Texture lookup
In a GLSL shader the thexture coordinates my be normalized which means that the size of the texture maps to the coordinates on the range $[0,1]$ in each dimension. By convention the the bottom left corner of an image has the coordinates $(0,0)$, whereas the top right corner has the value $(1,1)$ assigned. In order to perform pixel-index-wise one has to transform the lookup coordinates by $\frac{pixellocation_x}{image_{size_x}}$ for its x coordinate and similarly for its y coordinate. Since the zero frequency component of each fourier image was shifted towards the centre of the image, we have also a bias involved in our lookup which we have to subtract from the lookup-coordinate in order to perform the final lookup.

Transformations, Scalings
what is scaled?

Texture Blending
The final rendered color for each pixel is a weighted average of different color components, such as the diffraction color, the texture color and the diffuse color. In our shader the diffraction color is weighted by a constant $w_{diffuse}$. the texture color is once scales by a binary weight determined by the absolute value of the Fresnel Term F and once by $1 - w_{diffuse}$.

Algorithm 3.4 Texture Blending

$\alpha = (abs(F) > 1)?1 : 0$
$c_{out} = (1 - w_{diffuse}) * c_{diffraction} + (1 - \alpha) * c_{texture} + w_{diffuse} * c_{texture})$

Color Transformation
mention CIE XYZ to CIE RGB, D65, gamma correction.

3.5 Discussion

Our Current approach will sample the whole wavelength spectrum for each pixel but there is an optimization possible: Lets consider (u, v, w) defined as 2.16. Let d be the spacing between two slits of a grating. For any $L(\lambda) \neq 0$ it follows $\lambda_n^u = \frac{du}{n}$ and $\lambda_n^v = \frac{du}{n}$. For $n = 0$ there it follows $(u, v) = (0, 0)$. If $u, v > 0$

$$N_{min}^u = \frac{du}{\lambda_{max}} \leq n_u \leq \frac{du}{\lambda_{min}} = N_{min}^u$$
$$N_{min}^v = \frac{dv}{\lambda_{max}} \leq n_v \leq \frac{dv}{\lambda_{min}} = N_{min}^v$$

If $u, v < 0$

$$N_{min}^u = \frac{du}{\lambda_{min}} \leq n_u \leq \frac{du}{\lambda_{min}} = N_{max}^u$$
$$N_{min}^v = \frac{dv}{\lambda_{min}} \leq n_v \leq \frac{dv}{\lambda_{min}} = N_{max}^v$$

By transforming those equation to $(\lambda_{min}^u, \lambda_{min}^u)$, $(\lambda_{min}^v, \lambda_{min}^v)$ respectively for any (u, v, w) for each pixel we can reduce the number of required iterations in our shader.

Note: issue at center, specularity handled seperately. pq-apporach.

Kapitel 4

Evaluation Data Acquisition

4.1 Data Acquisition

For measurement on the true surface topography of snake sheds, samples are stuck on glass plates using double face tape, the animal was pushed up below a hollowed plate letting the skin emerging from the top of the plate. the surface of the scale under measurement should be large compared to the size of the drop to avoid wetting the plasmic membrane that would corrupt the reasing of the contact angle.

Measurements were carried out using intermittent contact mode in a Burker Dimension 3100 atomic force microscope (AFM) under ambient conditions using a Nanoscope V controller.

An AFM is a microscope that uses a tiny probe mounted on a cantilever to scan the surface of an object. The probe is extremely close tobut does not touchthe surface. As the probe traverses the surface, attractive and repulsive forces arising between it and the atoms on the surface induce forces on the probe that bend the cantilever. The amount of bending is measured and recorded, providing a map of the atoms on the surface. Atomic force microscopes can achieve magnification of a factor of 5×106, with a resolution of 2 angstroms, sufficient to resolve individual carbon atoms. Also called scanning force microscope. is a very high-resolution type of scanning probe microscopy, with demonstrated resolution on the order of fractions of a nanometer, more than 1000 times better than the optical diffraction limit.

The tops used were etched silicon TESP tips with a nominal frequency and force constant of 320 kHz and 42 N/m respectively.

SHOW AFM IMAGE

4.2 Diffraction Gratings

An idealised grating is made of a very large number of parallel, evenly spaced slits in an in an opaque sheet. Typically, it would have about 10,000 slits. In order to cause diffraction, the spacing between slits must be wider than the wavelength of interest. Each slit in the grating acts as a quasi point source from which light propagates in all directions. The diffracted light is composed of the sum of interfering wave components emanating from each slit in the grating.

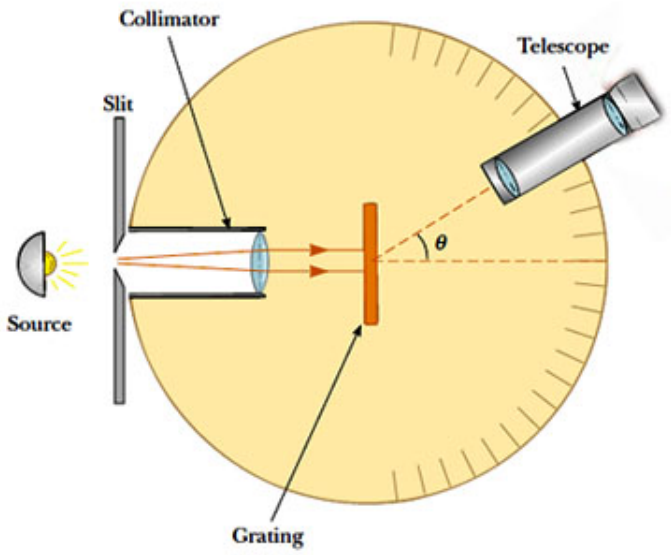

Abbildung 4.1: Spectometer: When a beam of monochromatic light passes through a grating placed in a spectrometer, images of the sources can be seen through the telescope at different angles.

Suppose monochromatic light is directed at the grating parallel to its axis as shown in figure. Let the distance between successive slits be equal d.

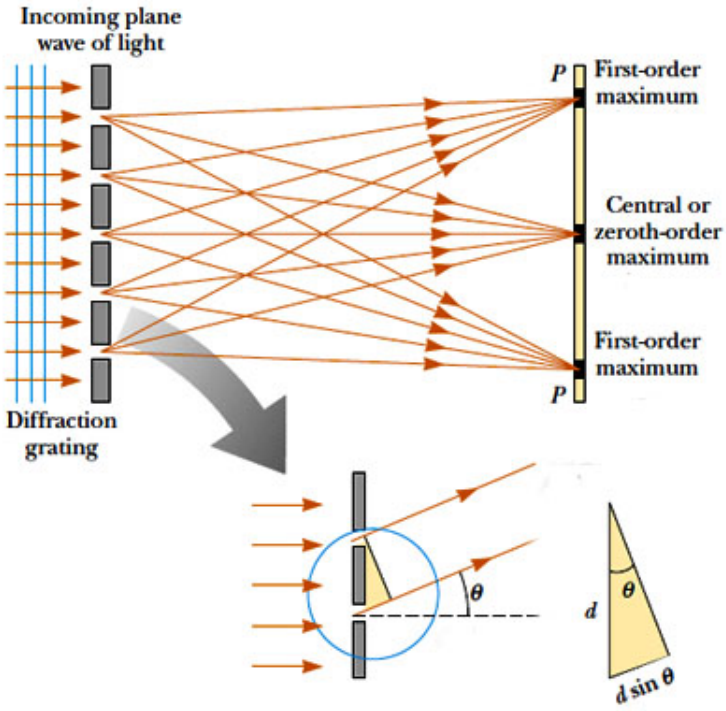

Abbildung 4.2: Light directed to parallel to grating:

The diffraction pattern on the screen is the result of the combined effects of diffraction and interference. Each slit causes diffraction, and the diffracted beams in turn interfere with one another to produce the pattern. The path difference between waves from any two adjacent slits can be found by dropping a perpendicular line between the parallel waves. By geometry, this path difference is $dsin(\theta)$. If the path difference equals one wavelength or some integral multiple of a wavelength, waves from all slits will be in phase and a bright line will be observed at that point. Therefore, the condition for maxima in the interference pattern at the angle θ is:

$$dsin(\theta) = m\lambda \tag{4.1}$$

where $m \in \mathbb{N}_0$ is the order of diffraction.

Because d is very small for a diffraction grating, a beam of monochromatic light passing through a diffraction grating is splitted into very narrow bright fringes at large angles θ.

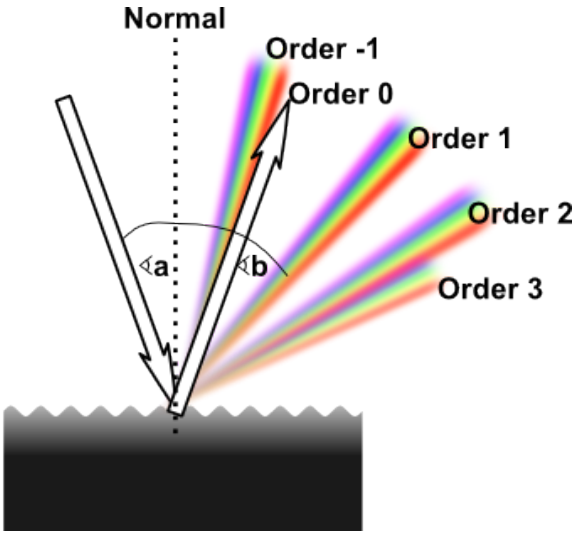

Abbildung 4.3: Different Orders of diffraction: When light is directed at the grating not parallel to its axis, there is another $sin(a)$ invovled. See grating equation 4.2.

When a narrow beam of white light is directed at a diffraction grating along its axis, instead of a monochromatic bright fringe, a set of coloured spectra are observed on both sides of the central white band as shown in figure 4.3.

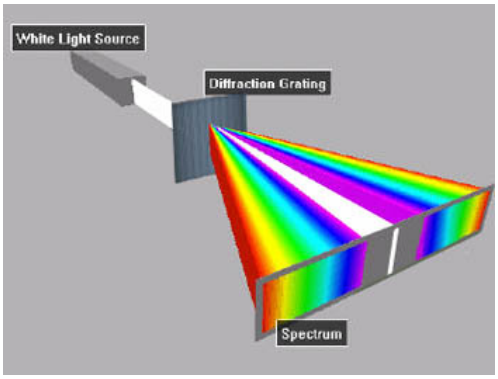

Abbildung 4.4: White Light beam causes coloured diffraction spectra

Since θ increases with wavelength λ, red light which has the longest wavelength is diffracted through the largest angle. Violet light has the shortest wavelength and is diffracted the least. Thus, white light is split into its component colours from violet to red light. The spectrum is repeated in the different orders of diffraction. Only the zeroth order spectrum is pure white.

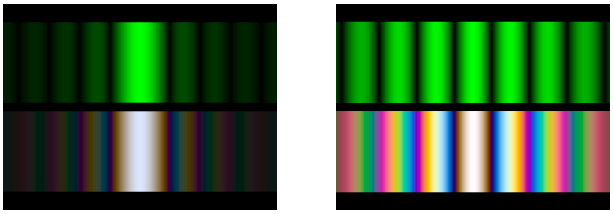

(a) one slits (b) two slits

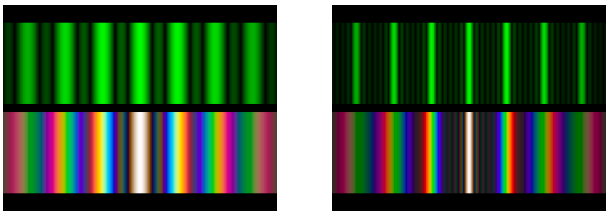

(c) three slits (d) seven slits

Abbildung 4.5: Difference of diffraction pattern between a monochromatic (top) and a white (bottom) light spectra for different number of slits.

4.3 Evaluation

UNIFY ANGLE NAMES:

In order to check the physical reliability of our method we applied it on a syntetic blazed grating, Elaphe and Xenopeltis snake sheds and evaluated its response using the grating equation. This equation models the relationship between the grating spacing and the angles of the incident and diffracted beams of light.

When light at a wavelength λ falls on a sample presenting a periodicity d along the incident plane under an incident angle θ compared to the normal of the surface the angle ϕ corresponding to the direction of the emerging beam showing constructive interferences (maximum in intensity) is given by the grating equation:

$$sin(\theta) = sin(\phi) + \frac{m\lambda}{d} \tag{4.2}$$

In our evaluation we are interested in the zero order diffraction, i.e. m equals zero which corresponds to direct transmission or specular reflection in the case of a reflection grating. Within our evaluation we further assume that the incident light direction w_i is given. In contrast the direction of the reflected wave w_r is not given. In Mathematics, a three dimensional direction vector is fully defined by two two angles, i.e. it can be represented by spherical coordinates with radius $r = 1$. By convention, we denote those two vectors by θ and ϕ. Hence, θ_i, ϕ_i and ϕ_r are given constants whereas θ_i is a free parameter for our evaluation simulation. Therefore, we are going to compare the maxima for peak viewing angle corresponding to each wavelength using data produced by our method against the maxima resulting by the grating equation.

4.3.1 Precomputation

SHOW IMAGE OF GRID

Before being able to compare the output produced by our method by the grating equation, we have to discretise the wavelength space Λ and the range Θ of our free parameter θ_i. We also have to initially assign θ_i, ϕ_i and ϕ_r. For our experiments we choose the following initial setup: $\theta_i = 75$ $\phi_i = 0$ $\phi_r = 180$ degree. Further we discretise the lambda space $\Lambda = \{\lambda | \lambda = \lambda_{min} + k\lambda_{step}, k \in \{0, .., C-1\}\}$ where $\lambda_{step} = \frac{\lambda_{max} - \lambda_{min}}{C-1}$ and C is the discretisation level of the lambda space, in our scenario $C = 42$. We similarly discretise the angle space by predefining an minimal and maximal angle boundary and $ceil(angMax - angMin)/angInc$ is the number of angles. We are going implement a similar algorithm as the diffraction fragment shader algorithme on the grid $[\Lambda, \Theta]$ and will store its spectral response in a matrix $R = \{response(\lambda_i, \theta_r^j) | iindex(\Lambda), jindex(\Theta)\}$. We also have evaluated our other shaders, mentioned within the discussion of the derivation and implementation chapters.

4.3.2 Data evaluation

Algorithm 4.1 Evaluation: lambda thetar graph

```
% load all variables computed in java
lInc = (lMax - lMin)./(lambdaCnt-1);
lambda = lMin + lInc*(-1+[1:lambdaCnt]);
[maxC maxI] = max(response.');
viewAngForMax = angMin + angInc * (maxI-1);
plot(lambda, viewAngForMax,'-r');s

for thetaI=baseAngle-eps:0.5:baseAngle+eps,
        % grating equation
        thetaV = asin(lambda./dPeriod - sin(thetaI*pi()/180))*180/pi();
        if(thetaI==75)
                plot(lambda, thetaV,'+ b');
        else
                plot(lambda, thetaV,'. g');
        end
end
```

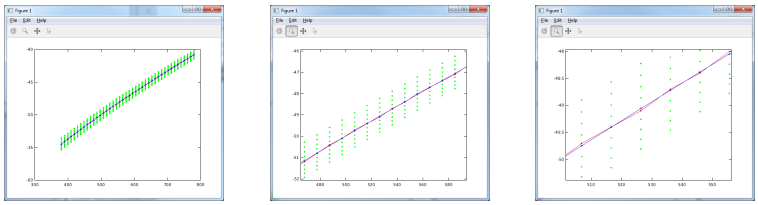

(a) plot λ - θ_i (b) Zoomed in (c) Further zoomed in

Abbildung 4.6: Evaluation: blaze grating

red graph is based on data produced by our method, the blue and green graphs are plots from the grating equation for different angles. If the blue graph is close the the red one, then our method performs well.

SHOW PLOTS AND TALK ABOUT THEM

subvariants: sample whole lambda space, just a few lambdas, pq approach. discussion

Kapitel 5

Results

show comparision between all shader variants: pq, adaptive, all, nvidiaGem.

show all views results. differece of this shader compared to evaluation shader show real snake images for comparison with real rendered images show experiments received show rendered images by daljits implemetation of stams approach. show our renderer's results mention all input parameters and their values. mention system specs and how long it took in order to precompute show some idft2 images, used patch, besids rendered image what initial size was used patch? mention GEM results. mention real results from geneva - use same paramter setup.

5.1 BRDF maps

ADD ALOT OF TEXT

(a) A (b) B

Abbildung 5.1: Species Elaphe Guttata

(a) A (b) B

Abbildung 5.2: Species Xenopeltis Unicolor

(a) Blaze grating (b) elaphe grating (c) xeno grating

Abbildung 5.3: BRDF maps for different patches

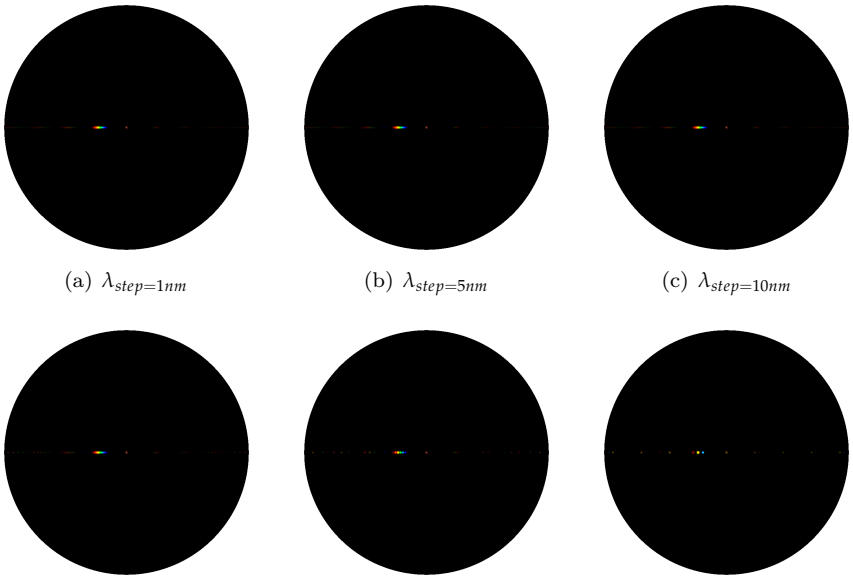

(a) $\lambda_{step=1nm}$ (b) $\lambda_{step=5nm}$ (c) $\lambda_{step=10nm}$

(d) $\lambda_{step=25nm}$ (e) $\lambda_{step=50nm}$ (f) $\lambda_{step=100nm}$

Abbildung 5.4: Blaze grating at $2.5\mu m$: Different λ step sizes

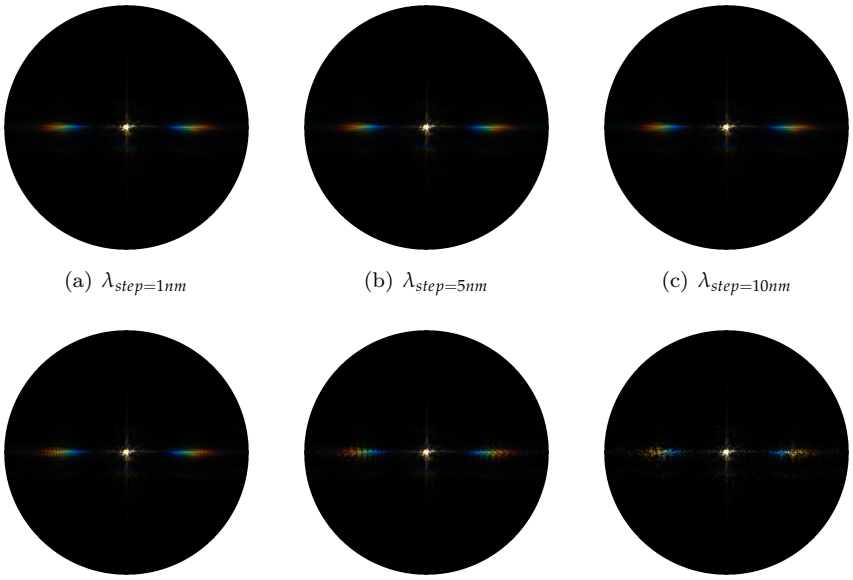

(a) $\lambda_{step=1nm}$ (b) $\lambda_{step=5nm}$ (c) $\lambda_{step=10nm}$

(d) $\lambda_{step=25nm}$ (e) $\lambda_{step=50nm}$ (f) $\lambda_{step=100nm}$

Abbildung 5.5: Elaphe grating at $65\mu m$: Different λ step sizes

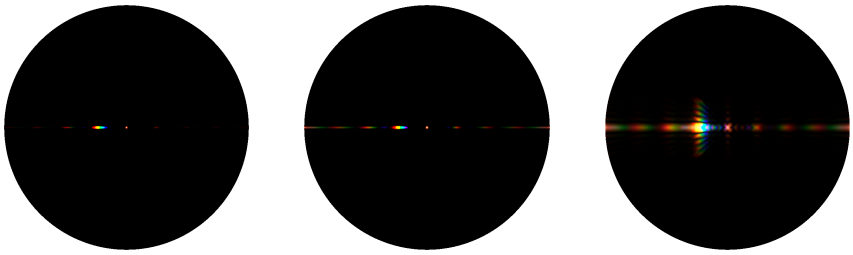

(a) Full Lambda Sampling: Blaze grating

(b) Full Lambda Sampling brightened: Blaze grating

(c) PQ Approach: Blaze grating

Abbildung 5.6: Blaze grating: PQ approach vs full lambda space sampling

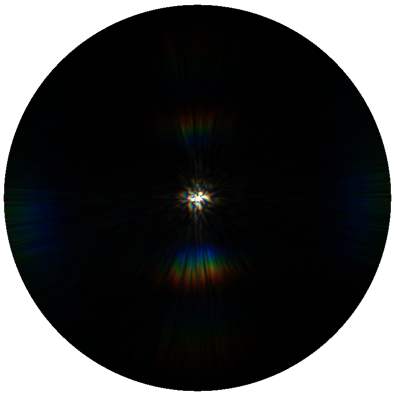

(a) Full Lambda Sampling: Xeno grating $\theta_i = 0degree$

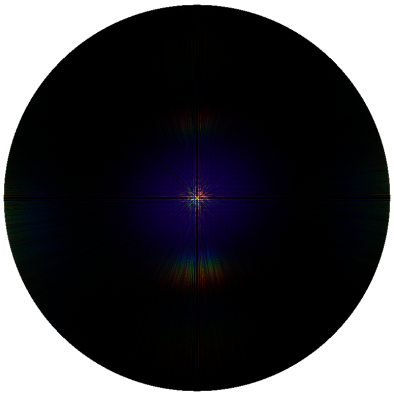

(b) PQ Approach: Xeno grating $\theta_i = 0degree$

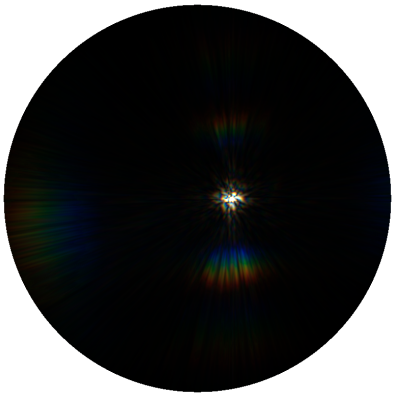

(c) Full Lambda Sampling: Xeno grating $\theta_i = 10degree$

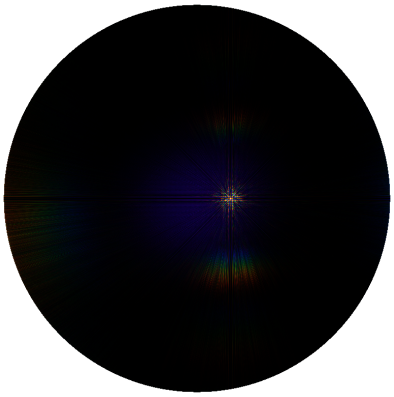

(d) PQ Approach: Xeno grating $\theta_i = 10degree$

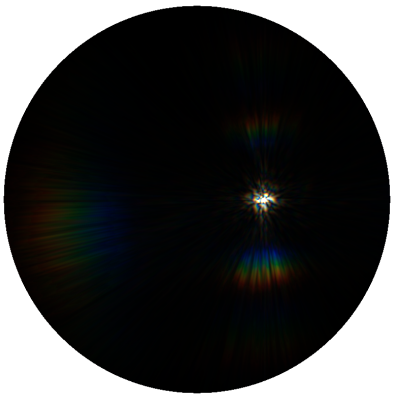

(e) Full Lambda Sampling: Xeno grating $\theta_i = 20degree$

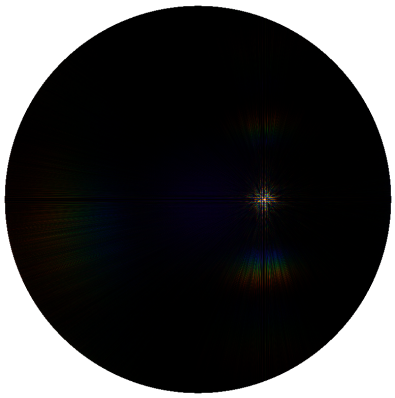

(f) PQ Approach: Xeno grating $\theta_i = 20degree$

Abbildung 5.7: Xeno grating: PQ approach vs full lambda space sampling

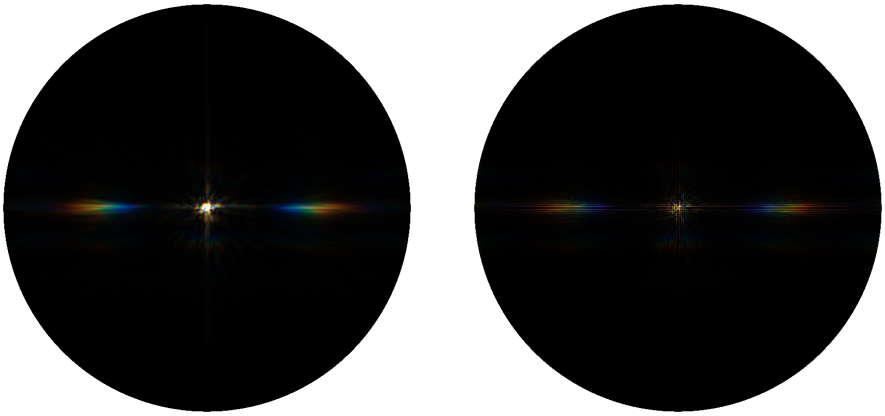

(a) Full Lambda Sampling: Elaphe grating (b) PQ Approach: Elaphe grating

Abbildung 5.8: Elaphe grating: PQ approach vs full lambda space sampling

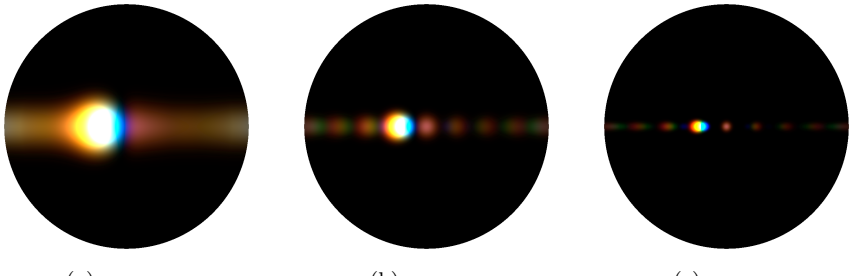

(a) $\sigma_{s=3.25\mu m}$ (b) $\sigma_{s=6.5\mu m}$ (c) $\sigma_{s=15\mu m}$

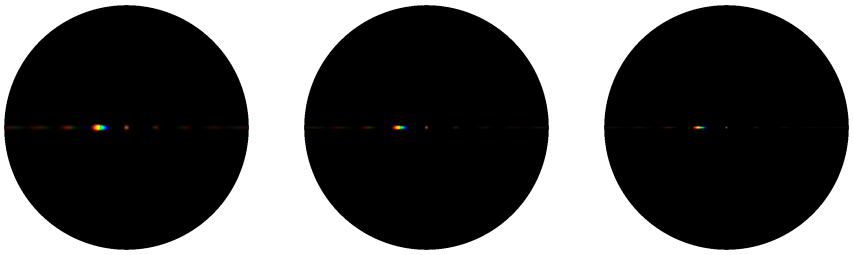

(d) $\sigma_{s=30\mu m}$ (e) $\sigma_{s=45\mu m}$ (f) $\sigma_{s=65\mu m}$

Abbildung 5.9: Blaze grating at $2.5\mu m$: Different σ_s sizes

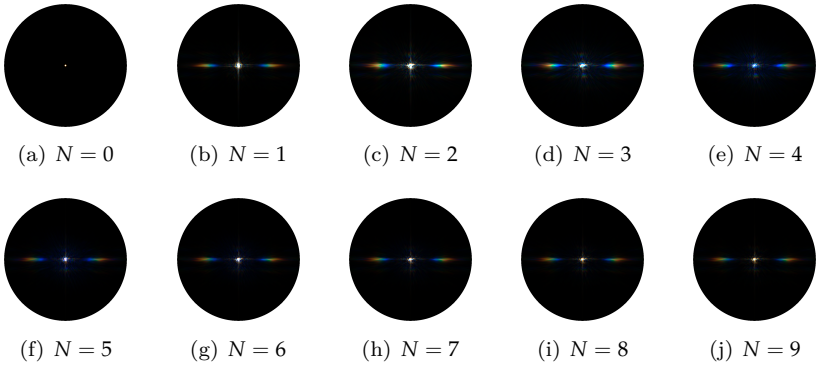

(a) $N = 0$ (b) $N = 1$ (c) $N = 2$ (d) $N = 3$ (e) $N = 4$

(f) $N = 5$ (g) $N = 6$ (h) $N = 7$ (i) $N = 8$ (j) $N = 9$

Abbildung 5.10: Elaphe grating at $65\mu m$: N Taylor Iterations

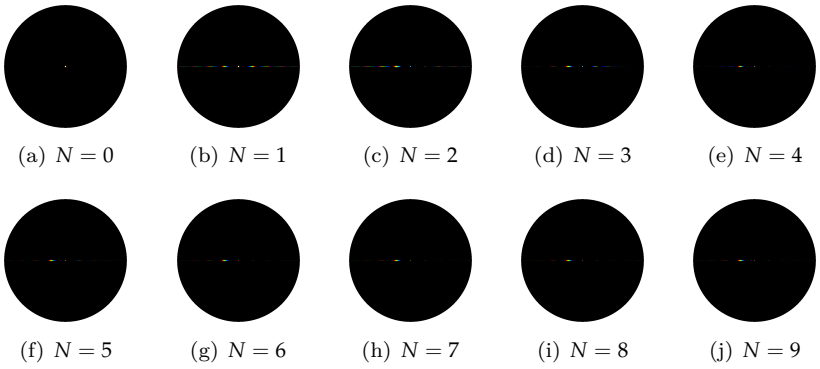

(a) $N = 0$ (b) $N = 1$ (c) $N = 2$ (d) $N = 3$ (e) $N = 4$

(f) $N = 5$ (g) $N = 6$ (h) $N = 7$ (i) $N = 8$ (j) $N = 9$

Abbildung 5.11: Blaze grating at $2.5\mu m$: N Taylor Iterations

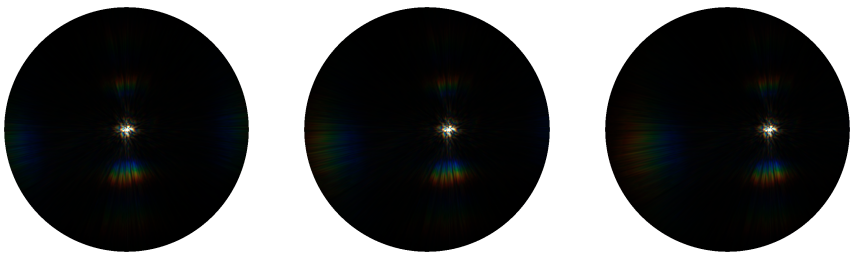

(a) Xeno grating $\theta_i = 0$ (b) Xeno grating $\theta_i = 10$ (c) Xeno grating $\theta_i = 20$

Abbildung 5.12: BRDF maps for Xeno grating: different θ_i angles

5.2 Snake surface geometries

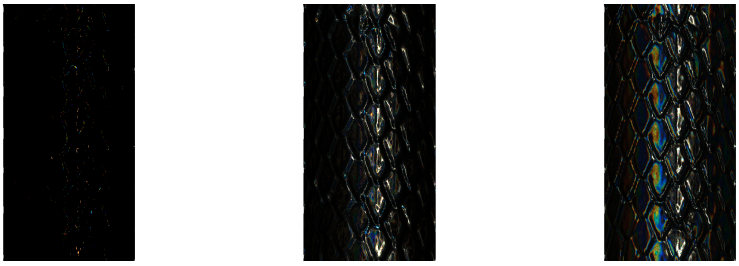

(a) Blaze grating (b) Elaphe grating (c) Xeno grating

Abbildung 5.13: Diffraction of different snake skin gratings rendered on a snake geometry

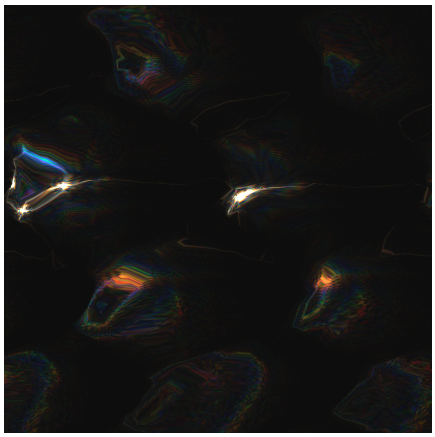

(a) $zoom = 0.1$

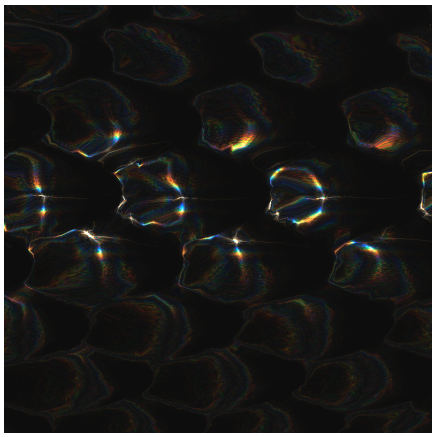

(b) $zoom = 0.2$

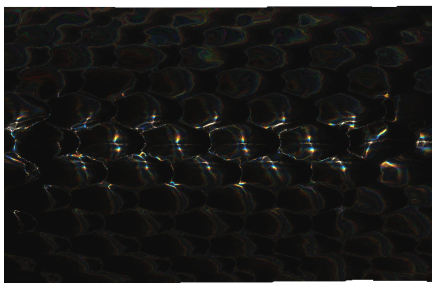

(c) $zoom = 0.5$

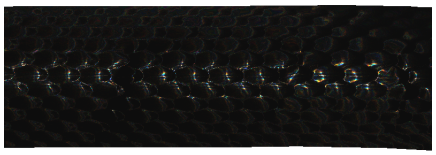

(d) $zoom = 1.0$

(e) $zoom = 1.5$

(f) $zoom = 2.0$

Abbildung 5.14: Diffraction on Elaphe snake skin grating: Different camera zoom levels

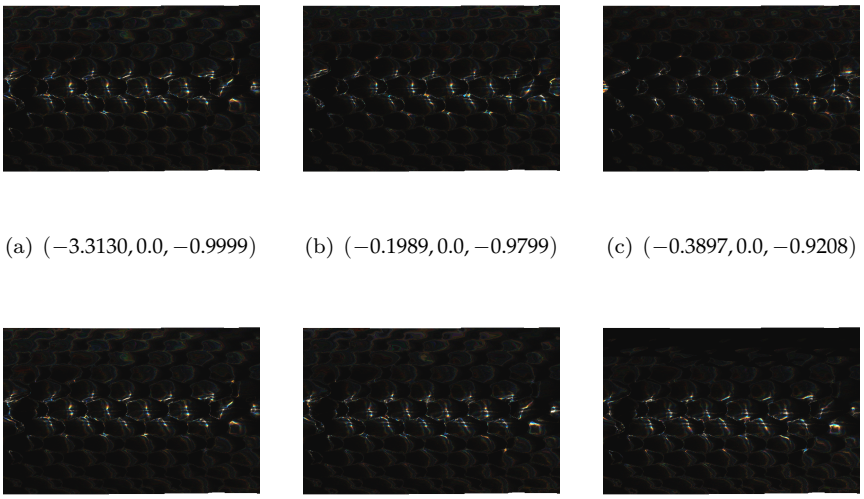

(a) $(-3.3130, 0.0, -0.9999)$ (b) $(-0.1989, 0.0, -0.9799)$ (c) $(-0.3897, 0.0, -0.9208)$

(d) $(0.0995, 0.0993, -0.9900)$ (e) $(0.0995, 0.2940, -0.9505)$ (f) $(0.0995, 0.4770, -0.8731)$

Abbildung 5.15: Diffraction on Elaphe snake skin grating: Different light directions

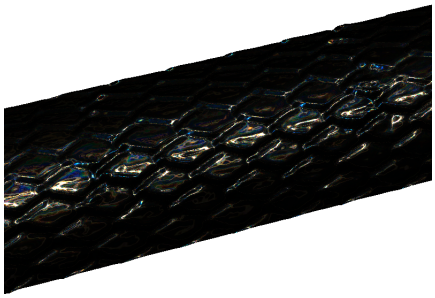

(a) Diffraction Patten

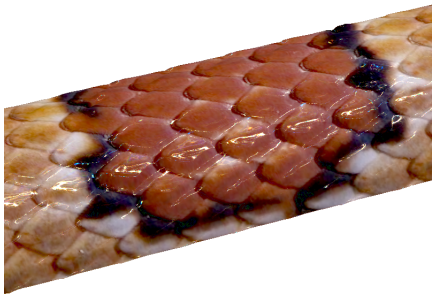

(b) Diffraction + Texture

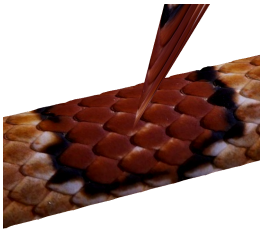

(c) Texture + Lightdir

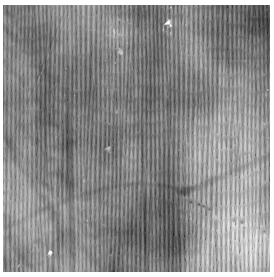

(d) Nanostructure

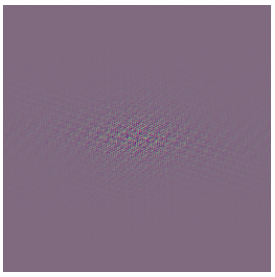

(e) Fourier Transform

Abbildung 5.16: Diffraction for Elaphe snake skin

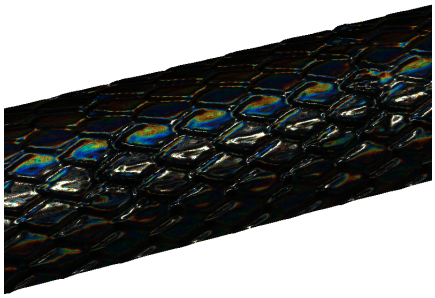

(a) Diffraction Patten

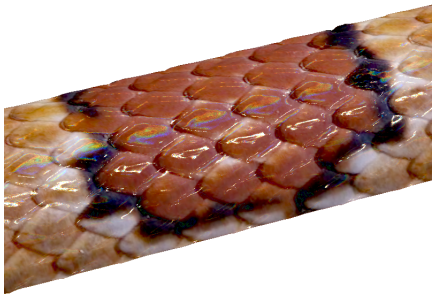

(b) Diffraction + Texture

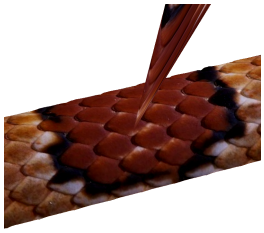

(c) Texture + Lightdir

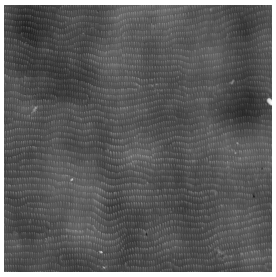

(d) Nanostructure

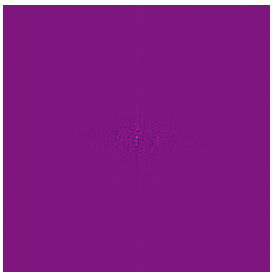

(e) Fourier Transform

Abbildung 5.17: Diffraction for Xeno snake skin

5.3 Snake surface geometries

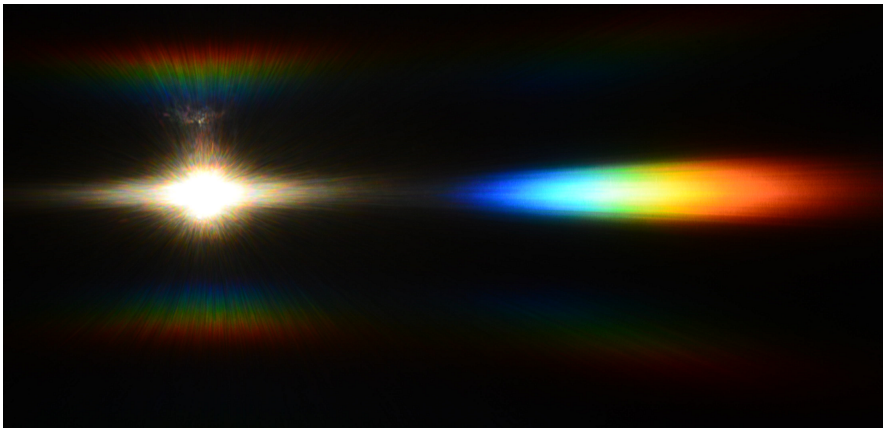

(a) Simulation

(b) Experiment

Abbildung 5.18: Diffraction Elpahe: simulation vs. experimental setup

Kapitel 6

Conclusion

can we do better?

brief overwiew pf results achieved, what was the most important in the work, appropriate to provide an introduction to possible future work in this field. reflect the emotions associated with the work, what was especially difficult or particularly interesting, one may elaborate on open questions within subjects related to the thesis without giving any answer. discuss follow-ups.

statment what you've researched and what your original contribution of the fild is explain why our approach is a good idea explain how the straight foreward approach would behave compared to our approach, computing the fourier transformations straight away. explain what we achieved, summary say something about draw-backs and about limitations of current apporach say something about the ongoing paper future work maybe say something about runtime complexity

6.1 Further Work

6.1.1 References

refs

6.2 Acknowledgment

Anhang A

Appendix

A.1 Schlick's approximation

The Fresnel's equations describe the reflection and transmission of electromagnetic waves at an interface. That is, they give the reflection and transmission coefficients for waves parallel and perpendicular to the plane of incidence. Schlick's approximation is a formula for approximating the contribution of the Fresnel term where the specular reflection coefficient R can be approximated by:

$$R(\theta) = R_0 + (1 - R_0)(1 - \cos\theta)^5 \tag{A.1}$$

and

$$R_0 = \left(\frac{n_1 - n_2}{n_1 + n_2}\right)^2$$

where θ is the angle between the viewing direction and the half-angle direction, which is halfway between the incident light direction and the viewing direction, hence $\cos\theta = (H \cdot V)$. And n_1, n_2 are the indices of refraction of the two medias at the interface and R_0 is the reflection coefficient for light incoming parallel to the normal (i.e., the value of the Fresnel term when $\theta = 0$ or minimal reflection). In computer graphics, one of the interfaces is usually air, meaning that n_1 very well can be approximated as 1.

A.2 Spherical Coordinates

$$\forall \begin{pmatrix} x \\ y \\ z \end{pmatrix} \in \mathbb{R}^3 : \exists r \in [0, \infty) \exists \phi \in [0, 2\pi] \exists \theta \in [0, \pi] \text{ s.t.}$$

$$\begin{pmatrix} x \\ y \\ z \end{pmatrix} = \begin{pmatrix} rsin(\theta)cos(\phi) \\ rsin(\theta)sin(\phi) \\ rcos(\theta) \end{pmatrix}$$

Tabellenverzeichnis

Abbildungsverzeichnis

List of Algorithms

Literaturverzeichnis

[Doe00] Doe, John: *Title*. Publisher, 0000. – ISBN 0000000000

Erklärung

gemäss Art. 28 Abs. 2 RSL 05

Name/Vorname: .....

Matrikelnummer: .....

Studiengang: ……

Bachelor ☐ Master ☐ Dissertation ☐

Titel der Arbeit: .....

.....

.....

LeiterIn der Arbeit: .....

.....

Ich erkläre hiermit, dass ich diese Arbeit selbständig verfasst und keine anderen als die angegebenen Quellen benutzt habe. Alle Stellen, die wörtlich oder sinngemäss aus Quellen entnommen wurden, habe ich als solche gekennzeichnet. Mir ist bekannt, dass andernfalls der Senat gemäss Artikel 36 Absatz 1 Buchstabe o des Gesetztes vom 5. September 1996 über die Universität zum Entzug des auf Grund dieser Arbeit verliehenen Titels berechtigt ist.

.....
Ort/Datum

.....
Unterschrift